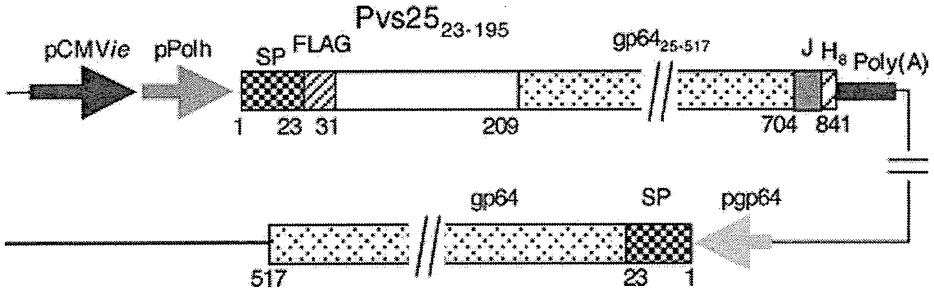

Fig. 1. Schematic representation of AcNPV-Dual-Pvs25 genome structure. A gene cassette that consisted of the gp64 signal sequence (SP), the *Pvs25* gene ($Pvs25_{25-195}$) fused to the N terminus of the AcNPV major envelope protein *gp64* gene ($gp64_{25-517}$), and the rabbit β-globlin poly(A) signal [poly(A)]. Expression of the gene cassette was driven by a dual promoter that consisted of the CMV immediate early enhancer/promoter (pCMV*ie*) and the polyhedrin promoter (pPolh). AcNPV-Dual-Pvs25 also possessed the endogenous *gp64* gene. Numbers indicate the amino acid positions of Pvs25–gp64 fusion protein and endogenous gp64. FLAG, FLAG epitope tag; $Pvs25_{25-195}$, Pvs25 corresponding to amino acids 25–195; $gp64_{25-517}$, gp64 corresponding to amino acids 25–517; J, junction consisting of 29 unrelated amino acid residues; H8, His-tag; pgp64, gp64 promoter.

For i.n. immunization, a total of 50 μl, divided into three doses delivered at 5-min intervals, was inoculated dropwise with a 20 μl pipette. As a comparative (negative) control, mice were immunized i.n. with 1×10^8 PFU of AcNPV-CMV-EGFP. Sera were collected two weeks after the final immunization prior to infection with *P. berghei* (either ANKA 2.34 or Pvs25DR3) to evaluate anti-Pvs25 response by ELISA. Immunized mice were kept for a total of 5 months following final immunization to quantify immune response over a longer time period. Serum was harvested from each mouse on a monthly basis, and ELISA performed as described below.

To prepare antibodies for use in standard membrane feeding assays using vivax patient blood, rabbits were immunized subcutaneously three times at 3-week intervals with 1×10^8 PFU of AcNPV-Dual-Pvs25. Two weeks after the final immunization, sera were collected and IgG purified using HiTrap™ Protein G HP chromatography (GE Healthcare) together with pre-immune rabbit sera.

2.6. ELISA for antibody titres and isotypes

Sera obtained from immunized mice were collected by tail bleeds prior to challenge. For some mice, sera were also collected periodically after final immunization. ELISA plates pre-coated with 100 ng/well GST-Pvs25 were incubated with serial dilutions of sera. Specific IgGs were detected using HRP-conjugated goat anti-mouse IgG (H + L) (Bio-Rad, Hercules, CA). For isotype determination, HRP-conjugated rabbit anti-mouse IgG1, IgG2a, IgG2b, and IgG3 (Zymed Laboratories, San Francisco, CA) antibodies were used. The plates were developed with peroxidase substrate solution [H_2O_2 and 2,2′-azino-bis(3-ethylbenzthiazoline-6-sulphonic acid)]. The OD at 414 nm of each well was measured using a plate reader. Endpoint titres were expressed as the reciprocal of the highest sample dilution for which the OD was equal or greater than the mean OD of non-immune control sera.

2.7. Transmission-blocking assay (standard membrane feeding assay)

Peripheral blood was collected from four volunteer patients infected only with *P. vivax* as described above. Purified anti-AcNPV-Dual-Pvs25 rabbit IgG was diluted (1-, 4- and 16-fold) with IgG from pre-immune rabbits, then 75 μl of each rabbit IgG mixture was mixed with 105 μl of heat-inactivated normal human AB serum prepared from malaria naive Thai donors. Diluted IgG was mixed with *P. vivax*-infected blood cells (1:1, v/v ratio) and incubated for 15 min at room temperature. The mixture was placed in a membrane feeding apparatus at 37 °C. *Anopheles dirus* A mosquitoes (Bangkok colony, Armed Forces Research Institute of Medical Sciences) were allowed to feed for 30 min. Unfed mosquitoes were removed after blood feeding, and fully engorged mosquitoes were maintained on 10% sucrose for seven days. For each diluted IgG, at least 20 mosquitoes were dissected and analyzed by staining with 0.5% mercurochrome and subsequent microscopy to count the number of oocysts that developed on the mosquito midguts.

2.8. Transmission-blocking assay (active immunization)

In three separate experiments, mice immunized i.m. or i.n. with AcNPV-Dual-Pvs25 were divided into two groups (three mice per group), PH treated, and three days later infected i.p. with 10^6 parasites of *P. berghei* ANKA 2.34 or *P. berghei* Pvs25DR3. As a negative control, mice were immunized i.n. with AcNPV-CMV-EGFP, divided into two groups and infected as above. Three days post-infection, starved *A. stephensi* mosquitoes were allowed to feed on the infected mice. In all pots, >50 fed mosquitoes were fed per mouse. 24 h after feeding, mosquitoes were briefly anesthetized with CO_2, and unfeds removed. Mosquitoes were then maintained on fructose [8% (w/v) fructose, 0.05% (w/v) *p*-aminobenzoic acid] at 19–22 °C and 50–80% relative humidity. Day 10 post-feeding, mosquito midguts were dissected, and oocyst prevalence and intensity recorded. All care and handling of animals was in accordance with the Guidelines for Animal Care and Use prepared by Jichi Medical University and Imperial College London.

2.9. Statistical analyses

Statistical analysis was performed with Graphpad Prism Software (Graphpad Software Inc.). For the membrane feeding assay, The Kruskal–Wallis test was used to examine the difference in oocyst counts per mosquito between pre-immune IgG and immune IgG groups. For long-term anti-Pvs25 ELISA responses, significant variations of titres over time were evaluated using Spearman's rank correlation ($p < 0.05$). For active immunization, significance was assessed using Mann–Whitney *U* test (to examine the difference in oocyst counts per mosquito between AcNPV-Dual-Pvs25 or AcNPV-CMV-EGFP immunized groups) and the Fisher's exact probability test (to examine the difference in infection prevelance between AcNPV-Dual-Pvs25 or AcNPV-CMV-EGFP immunized groups) *P* values less than 0.05 were considered statistically significant.

3. Results

3.1. Construction of baculovirus-based Pvs25 vaccine

To examine the expression of conformation-dependent epitopes, AcNPV-Dual-Pvs25 viral particles were analyzed by

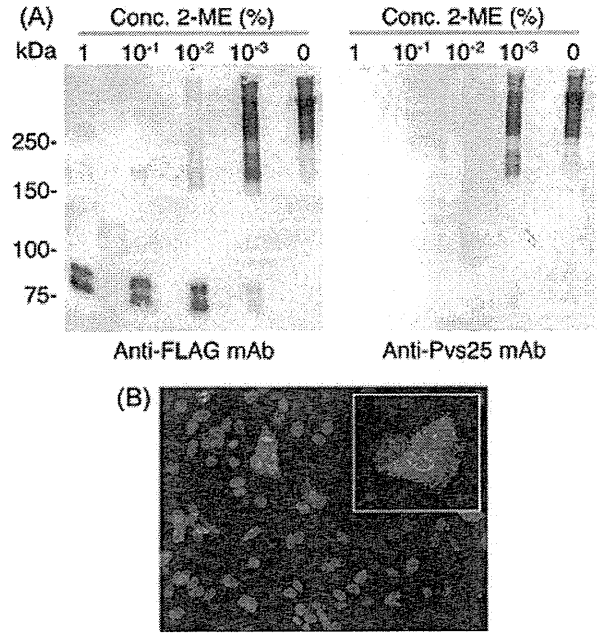

Fig. 2. Expression of Pvs25–gp64 fusion protein. (A) Western blotting of AcNPV-Dual-Pvs25 in the presence of various concentrations of 2-ME. AcNPV-Dual-Pvs25 was treated with the loading buffer containing descending concentrations of 2-ME. Reactivity of $Pvs25_{25-195}$ fusion protein was examined using either anti-FLAG mAb or anti-Pvs25 mAb, N1-1H10. The concentrations of 2-ME are shown above the gel. (B) *In vitro* expression analysis of Pvs25 by transducing AcNPV-Dual-Pvs25 in mammalian cells. HepG2 cells were transduced with AcNPV-Dual-Pvs25 at an m.o.i. of 10. Forty-eight hours later, cells were fixed with 5% paraformaldehyde followed by permeabilization with 0.1% Triton X in PBS, and incubated with anti-Pvs25 mAb 1H10. Bound antibodies were detected by FITC-labeled anti-mouse IgG by fluorescence microscopy (green). Cell nuclei were visualized by DAPI staining (blue). Original magnification, ×400.

Western blotting in the absence or presence of 10^{-3}% to 1% 2-mercaptoethanol (2-ME) (Fig. 2A). Anti-FLAG mAb, which recognizes a linear epitope within the N-terminal tag, reacted with doublet bands at all 2-ME concentrations, with relative molecular masses (M_r) of 80 and 90 kDa. The 80 kDa band corresponded to the predicted M_r of the Pvs25–gp64 fusion protein (Fig. 2A, left panel). We hypothesise the 90 kDa band may have resulted from post-translational modification within the insect cells. When 2-ME is added at concentrations above 10^{-3}%, recognition by anti-Pvs25 mAb N1-1H10, which has previously been shown to recognize a conformation-dependent epitope [29], is not detectable. In contrast, reducing of the concentration of 2-ME to below 10^{-3}% increased the reactivity of Pvs25–gp64 fusion protein with the mAb (Fig. 2A, right panel). These results suggest that the Pvs25–gp64 fusion protein on the virus envelope retains components of the three-dimensional structure of native Pvs25 protein, important to antibody recognition.

We also examined by IFA the ability of AcNPV-Dual-Pvs25 to drive Pvs25 expression in mammalian cells. Strong immunofluorescence signals were detected with N1-1H10 mAb in HepG2 cells infected with AcNPV-Dual-Pvs25 48 h after transfection (Fig. 2B). Thus AcNPV-Dual-Pvs25 not only expressed appropriately folded Pvs25 on viral particles, but also in mammalian cells.

3.2. Immunization with AcNPV-Dual-Pvs25 induces high Pvs25-specific antibody titres

I.n. and i.m. immunization with AcNPV-Dual-Pvs25 induced high antibody titres (>1:15,000) (Fig. 3A). Pvs25 antibodies were predominately IgG1, IgG2a and IgG2b (IgG1:IgG2a ratio ≅0.12 and 0.29 for i.m. and i.n. immunizations, respectively), indicating a mixed Th1/Th2-type immune response. IgG2b, which is inducible by mucosal immunization, was significantly higher in the i.n. group than the i.m. group. As demonstrated by the IFA test, these immune sera strongly reacted with Pvs25 in its native location on the parasite surface, circumferential staining of the *P. vivax* retort-form ookinete was prominent (Fig. 3B). Pvs25-specific antibody titres in sera obtained from both the i.m. and i.n. AcNPV-Dual-Pvs25 groups were sustained without any significant reduction over 5 months following the final immunization (Fig. 4).

3.3. Evaluation of transmission-blocking activity (SMFA)

Following subcutaneous immunization with AcNPV-Dual-Pvs25, IgG purified from immune rabbit serum reduced the intensity and prevalence of oocyst infection on the mosquito midgut profoundly (Fig. 5), in a dose-dependent manner. At an immune IgG concentration of 0.17 mg/ml, the mean intensity observed was 73.9 oocysts/midgut, and at 2.67 mg/ml, intensity was reduced to just 1.5 oocysts/midgut (a 98% inhibition of intensity when compared to pre-immune IgG at 2.67 mg/ml). Prevalence of infection was reduced by 70% from 94% in the pre-immune control, to give an overall reduction of 25.5% (with respect to pre-immune IgG). At lower concentrations of immune IgG tested, no significant reduction of prevalence was observed.

3.4. Evaluation of transmission-blocking activity (in vivo evaluation)

To examine transmission blockade *in vivo*, immunized mice were infected with transgenic *P. berghei* expressing Pv25 (Pvs25DR3), *A. stephensi* mosquitoes were fed directly on the immunized and challenged hosts (Table 1). AcNPV-Dual-Pvs25 was administered either by i.m. or i.n. route into six mice each. Six control mice were also immunized i.n. with AcNPV-CMV-EGFP as a negative control. For each immunization method, three mice were challenged with *P. berghei* ANKA 2.34 (to determine whether there was a direct but unexpected anti-*P. berghei* response), and three were immunized with *P. berghei* Pvs25DR3. WT *P. berghei* 2.34 does not express Pvs25, and any TB effect observed would be due to non-specific phenomenon. *P. berghei* Pvs25DR3 expresses Pvs25 on the zygote and ookinete surface [12]. Mosquitoes that fed on control (AcNPV-CMV-EGFP) mice immunized by the intranasal route displayed an, average intensity of infection of 2.16 oocysts/midgut (±S.E.M.), whereas following mucosal delivery of AcNPV-Dual-Pvs25 and subsequent challenge, the average intensity was significantly reduced to 0.17 oocysts/midgut (±S.E.M.). Following intramuscular delivery, intensity was 0.25 oocysts/midgut (±S.E.M.); thus achieving a 92.1% and an 88.4% inhibition of intensity of infection with intranasal and intramuscular deliveries, respectively. Prevalence was similarly reduced, by 83.8% and 75.5% respectively.

4. Discussion

The Baculovirus Dual Expression System aims to facilitate the development of multifunctional vaccines capable of inducing strong humoral and cellular immune responses without the need for extraneous immunological adjuvants. In the present study, we applied this system to generation of a novel *P. vivax* TBV (AcNPV-Dual-Pvs25), which possesses a single gene cassette that consists of the Pvs25–gp64 fusion gene under the CMV-polyhedrin dual promoter. AcNPV-Dual-Pvs25 not only displayed Pvs25 on the viral envelope but also expressed following transduction of mammalian cells. Immunization of mice with AcNPV-Dual-Pvs25 induced high Pvs25-specific antibody titres with predominant IgG1, IgG2a and

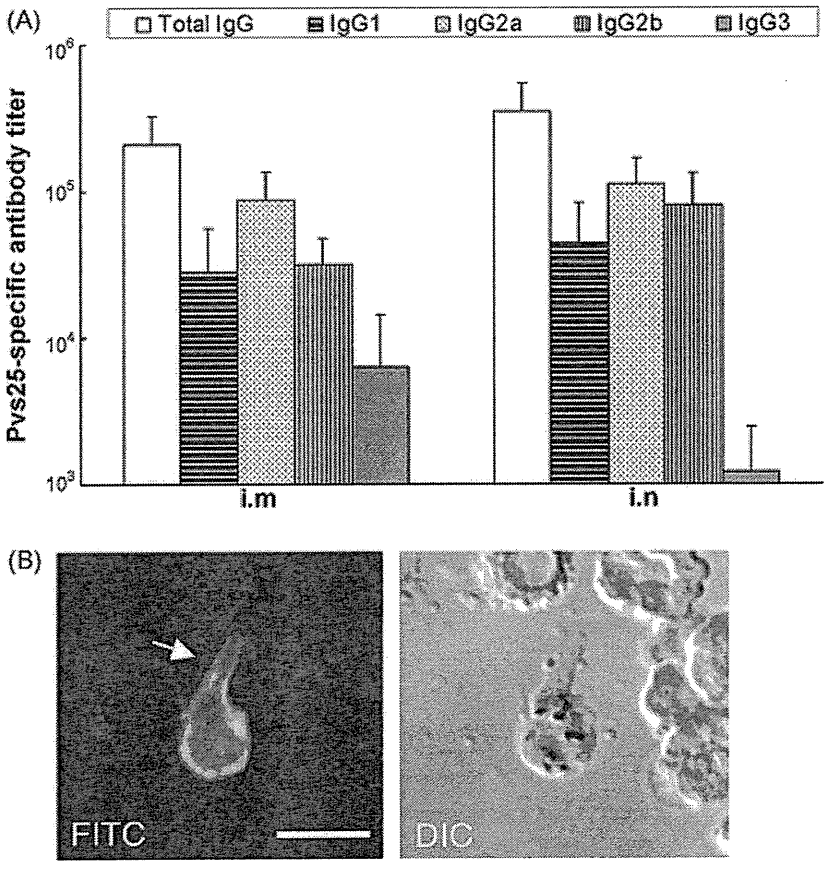

Fig. 3. Pvs25-specific antibody responses. Sera were collected from individual mice (6 mice/group) three weeks after the final immunization. (A) The individual sera were tested for total IgG, IgG1, IgG2a, IgG2b and IgG3 specific for Pvs25 by ELISA. The data represent one of two experiments, which had similar results. Data are the mean ± S.E.M. of groups. Significant differences of total IgG titres between different groups were evaluated using the two-tailed Fisher's exact probability test. *, $p < 0.01$. (B) Confocal fluorescence microscopy of sera obtained from mice immunized with AcNPV-Dual-Pvs25. The entire surface of cultured retorts/zygotes was clearly stained (green) by serum (1:500 dilution) obtained from a mouse immunized i.n. with AcNPV-Dual-Pvs25. Cell nuclei were visualized by blue DAPI staining (arrow) (immunofluorescence assay [IFA]). Right panel represents image obtained by differential interference contrast (DIC) microscopy. Scale bar, 10 μm.

IgG2b isotypes, indicating induction of both a mixed Th1/Th2 response.

We evaluated the transmission-blocking immunogenicity of AcNPV-Dual-Pvs25 using two methods. One was SMFA on peripheral blood from *P. vivax* infected patients. It has widely been accepted that malaria transmission-blocking immunity is mediated by antibodies that inhibit parasite development in the mosquito midgut [15,23,31,32]. The SMFA has provided valuable insights into functional transmission-blocking activities of sera from immunized animals. However, blood from *P. vivax*-infected patients as a source of SMFA is an unpredictable, and uncontrollable source of parasites and useful *in vitro* gametocyte culture has not been established. The other method was active immunization of mice followed by challenge with transgenic *P. berghei* Pvs25DR3. Compared with SMFA, active immunization/challenge method can assess the *in vivo* transmission-blocking potential of all immune factors including not only antibodies but also cytokine, complement and antibody-dependent cell cytotoxity. The approach of using transgenic rodent malarial parasites to assess the immune system's response to targets from a human malarial parasite has been described in previous studies [12–14]. Whilst the infectivity of all Pvs25DR3 transgenic lines tested to date is low compare to WT *P. berghei*, oocyst intensities are close to that seen *in vivo* for both *P. vivax* (and *P. falciparum*), and provide a very sensitive context to measure any transmission-blocking effect. Importantly, the transmission-blocking assays used clearly demonstrated that immunization with AcNPV-Dual-Pvs25 induced a strong transmission-blocking response, namely >90% reduction in oocyst number, and a corresponding fall in prevalence of 25.5% (SMFA) and 83.8% (i.n.)/75.5% (i.m.) (active immunization). These results provide support for this novel strategy for the delivery of a malarial TBV.

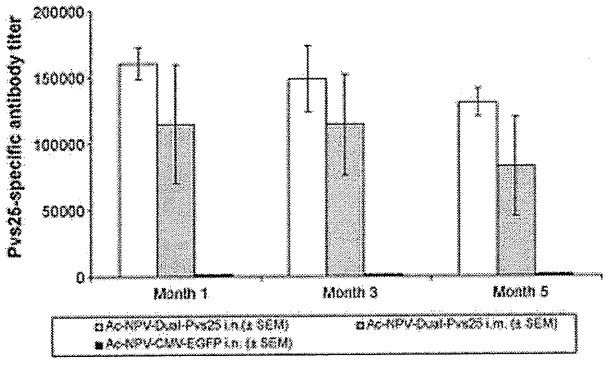

Fig. 4. Long-term ELISA titres following immunization with AcNPV-Dual-Pvs25. Sera were collected from individual mice three weeks following final immunization, and then at monthly intervals for 5 months. Six mice were examined for each immunogen. The individual sera were tested for total IgG specific for recombinant Pvs25 by ELISA. Samples shown are mean titres observed from six mice. Error bars show S.E.M. Significant variations of titres over time were evaluated using Spearman's rank correlation ($p < 0.05$). No statistically significant variation was observed in groups over 5 months.

Table 1
Evaluation of transmission-blocking activity by active immunization.

		Mean intensity (±S.E.M.)	Mean prevalence (% mosquitoes infected) (±S.E.M.)
AcNPV-Dual-Pvs25 immunized mice—i.n. delivery			
Mice 1–3: Pvs25DR3 challenged (±S.E.M.)		0.17 (0.1)	10.7 (3.1)
Mice 4–6: WT 2.34 challenged (±S.E.M.)		112.9 (8.43)	93.8 (3.46)
AcNPV-Dual-Pvs25 immunized mice—i.m. delivery			
Mice 7–9: Pvs25DR3 challenged (±S.E.M.)		0.25 (0.06)	16.2 (1.27)
Mice 10–12: WT 2.34 challenged (±S.E.M.)		88.8 (11.2)	89.6 (4.7)
AcNPV-CMV-EGFP immunized mice—i.n. delivery (negative control)			
Mice 13–15: Pvs25DR3 challenged (±S.E.M.)		2.16 (0.2)	66(4.23)
Mice 16–18: WT 2.34 challenged (±S.E.M.)		87.41 (15.6)	82.6 (10.9)
		Mean change in intensity	Mean change in prevalence
Overall Transmission blockade in AcNPV-Dual-Pvs25 immunised mice			
I.n.	Pvs25DR3	−92.10%[a]	−83.80%[b]
	P. berghei 2.34	+29.70%	+13.60%
I.m.	Pvs25DR3	−88.40%[a]	−75.50%[b]
	P. berghei 2.34	+1.60%	+8.50%

Mice were immunized four times with AcNPV-Dual-Pvs25 (i.m. and i.n.) or AcNPV-CMV-EGFP (i.n. only, negative control). Three groups of immunized mice were sub-divided into two groups, each containing three mice. Each group was then and challenged with WT *P. berghei* 2.34 (3 mice) or *P. berghei* Pvs25DR3 (3 mice), and used to assess transmission to mosquitoes via direct gametocyte feed. 10^6 parasites were injected per mouse. Mosquito midguts were dissected 10–12 days post feed. Mean intensities and prevalence were calculated from triplicate mice. Overall transmission blockade (in terms of both infection intensity and prevelance) was calculated by comparison to AcNPV-CMV-EGFP immunized mice. Significance was assessed using Mann–Whitney *U* test (to examine the difference in oocyst counts per mosquito between AcNPV-Dual-Pvs25 or AcNPV-CMV-EGFP immunized groups) and the Fisher's exact probability test (to examine the difference in infection prevelance between AcNPV-Dual-Pvs25 or AcNPV-CMV-EGFP immunized groups) ($p < 0.05$). Following challenge with WT *P. berghei* 2.34, no significant change in either intensity or prevalence was observed with either intranasal or intramuscular immunization. Significant inhibition was only observed following challenge with Pvs25DR3.

[a] $P < 0.05$, Mann–Whitney *U* test.

[b] $P < 0.05$, Fisher's exact probability test.

Mucosal vaccines have several attractive features compared with parenteral vaccines (e.g., safety, cost-effectiveness and ease of administration), but studies on their use have been limited almost exclusively to protection against mucosally transmitted pathogens. We provide evidence that i.n. immunization is a feasible alternative for preventing malaria, which is transmitted through non-mucosal routes. Compared with i.m. immunization, i.n. immunization led to higher Pvs25-specific antibody titres and potent transmission-blocking activity (i.n.:i.m.; intensity = 92.1%:88.4%, prevalence = 83.8%:75.5%). These results are consistent with our previous work showing that intranasal immunization with the baculovirus-based vaccine induced strong systemic humoral immune responses with high titres of antigen-specific antibodies and conferred complete protection against malaria blood-stage challenge [8,9,28]. It has previously been reported that intranasal immunization with recombinant Pvs25, using cholera toxin (CT) as an adjuvant, induced a systemic immune response with transmission-blocking activity [21]. Additionally, the mucosal immunogenicity and protective efficacy of recombinant Pfs25 and Pys25 have been thoroughly described [10,11]. CT, whilst a strong immune potentiator [10,11,21], which can induce immunological memory against heterologous antigens in a rodent model; however, it is precluded from clinical use due to its enterotoxicity and potential hazardous effects on olfactory nerves [22]. In contrast, a baculovirus-based delivery system may offer an attractive immunization method, as AcNPV exhibits low cytotoxicity and is incapable of replication in mammalian cells [8,9].

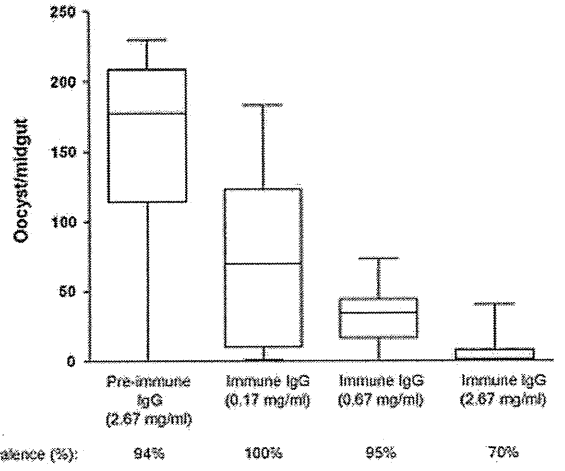

Fig. 5. Transmission-blocking efficacy against Thai *P. vivax* isolates by membrane feeding assay. Rabbits were immunized subcutaneously with AcNPV-Dual-Pvs25 vaccine. The purified rabbit IgG was evaluated by membrane feeding of *P. vivax*-infected blood from patients in Thailand. The IgG effectively inhibited oocyst formation in the mosquito midguts in a dose-dependent manner. Experiments were performed using blood from four volunteers naturally infected with *P. vivax*. The data presented was obtained from one volunteer. Data are expressed as the median numbers of oocysts per mosquitoes (lines in boxes), quartiles (boxes), and ranges (lines above and below boxes). Stastistically significant differences in oocyst counts per mosquito between pre-immune IgG and immune IgG groups were confirmed by the Kruskal–Wallis test ($P < 0.0001$).

Anti-malarial transmission-blocking vaccines based on the surface of the sexual and other sporogonic stages of *Plasmodium* inhibit further development of the parasite within the mosquito host, and have a significant potential to reduce malarial transmission in endemic areas. The data described here adds to previously presented data showing the significant potential of the baculovirus dual expression system against the blood stages of the parasite [8,9,28], but also demonstrates clearly its ability to induce antibodies against the ookinete surface protein Pvs25, and to elicit a transmission-blocking immune response against the *P. vivax* isolates from endemic areas, and a transgenic rodent malaria parasite model in preliminary studies.

Acknowledgments

We would like to thank Hitomi Araki for excellent assistance with the ELISAs and handling of the mice. We also thank Ken

Baker and Mark Tunnicliff for mosquito rearing (Imperial College, London). This work was supported by grants from the Ministry of Education, Culture, Sports and Science of Japan (21390126) (Jichi Medical University), and Biomalpar, Transmolbloc and BBSRC (award number LDAD_P15820) (Imperial College, London).

References

[1] Daly TM, Long CA. A recombinant 15-kilodalton carboxyl-terminal fragment of *Plasmodium yoelii yoelii* 17XL merozoite surface protein 1 induces a protective immune response in mice. Infect Immun 1993;61:2462–7.
[2] Davies AH. "Baculophage": a new tool for protein display. Biotechnology (N Y) 1995;13:1046.
[4] Jin R, Lv Z, Chen Q, Quan Y, Zhang H, Li S, et al. Safety and immunogenicity of H5N1 influenza vaccine based on baculovirus surface display system of *Bombyx mori*. PLoS ONE 2008;3:e3933.
[6] Matsuura Y, Possee RD, Overton HA, Bishop DH. Baculovirus expression vectors: the requirements for high level expression of proteins, including glycoproteins. J Gen Virol 1987;68(Pt 5):1233–50.
[8] Yoshida S, Kawasaki M, Hariguchi N, Hirota K, Matsumoto M. A baculovirus dual expression system-based malaria vaccine induces strong protection against *Plasmodium berghei* sporozoite challenge in mice. Infect Immun 2009;77:1782–9.
[9] Yoshida S, Kondoh D, Arai E, Matsuoka H, Seki C, Tanaka T, et al. Baculovirus virions displaying *Plasmodium berghei* circumsporozoite protein protect mice against malaria sporozoite infection. Virology 2003;316:161–70.
[10] Arakawa T, Tachibana M, Miyata T, Harakuni T, Kohama H, Matsumoto Y, et al. Malaria ookinete surface protein-based vaccination via the intranasal route completely blocks parasite transmission both in passive and active vaccination regimes in a rodent malaria infection model. Infect Immun 2009. E-pub ahead of print 14th Sep.
[11] Arakawa T, Komesu A, Otsuki H, Sattabongkot J, Udomsangpetch R, Matsumoto Y, et al. Nasal immunization with a malaria transmission-blocking vaccine candidate, Pfs25, induces complete protective immunity in mice against field isolates of *Plasmodium falciparum*. Infect Immun 2005;73(11):7375–80.
[12] Ramjanee S, Robertson JS, Franke-Fayard B, Sinha R, Waters AP, Janse CJ, et al. The use of transgenic *Plasmodium berghei* expressing the *Plasmodium vivax* antigen P25 to determine the transmission-blocking activity of sera from malaria vaccine trials. Vaccine 2007;25(January (5)):886–94.
[13] Mlambo G, Maciel J, Kumar N. Murine model for assessment of *Plasmodium falciparum* transmission-blocking vaccine using transgenic *Plasmodium berghei* parasites expressing the target antigen Pfs25. Infect Immun 2008;76(May (5)):2018–24.
[14] Kumar KA, Oliveira GA, Edelman R, Nardin E, Nussenzweig V. Quantitative *Plasmodium* sporozoite neutralization assay (TSNA). J Immunol Methods 2004;292(September (1–2)):157–64.
[15] Kaslow DC. Transmission blocking vaccines. In: Hoffman SL, editor. Malaria vaccine development. Washington, DC: ASM Press; 1996. p. 181–228.
[16] Hisaeda H, Collins WE, Saul A, Stowers AW. Antibodies to *Plasmodium vivax* transmission-blocking vaccine candidate antigens Pv25 and Pvs28 do not show synergism. Vaccine 2001;20(5–6):763–70.
[17] Peiris JS, Premawansa S, Ranawaka MB, Udagama PV, Munasinghe YD, Nanayakkara MV, et al. Monoclonal and polyclonal antibodies both block and enhance transmission of human *Plasmodium vivax* malaria. Am J Trop Med Hyg 1988;39(July (1)):26–32.
[18] Carter R. Transmission blocking malaria vaccines. Vaccine 2001;19(March (17–19)):2309–14.
[19] Malkin EM, Durbin AP, Diemert DJ, Sattabongkot J, Wu Y, Miura K, et al. Phase I clinical trial of Pvs25H: a transmission blocking vaccine for *Plasmodium vivax* malaria. Vaccine 2005;23:3131–8.
[20] Stowers A, Carter R. Current developments in malaria transmission-blocking vaccines. Expert Opin Biol Ther 2001;1:619–28.
[21] Arakawa T, Tsuboi T, Kishimoto A, Sattabongkot J, Suwanabun N, Rungruang T, et al. Serum antibodies induced by intranasal immunization of mice with *Plasmodium vivax* Pvs25 co-administered with cholera toxin completely block parasite transmission to mosquitoes. Vaccine 2003;21(July (23)):3143–8.
[22] Hagiwara Y, Iwasaki T, Asanuma H, Sato Y, Sata T, Aizawa C, et al. Effects of intranasal administration of cholera toxin (or Escherichia coli heat-labile enterotoxin) B subunits supplemented with a trace amount of the holotoxin on the brain. Vaccine 2001;19(February (13–14)):1652–60.
[23] Tirawanchai N, Winger LA, Nicholas J, Sinden RE. Analysis of immunity induced by the affinity-purified 21-kilodalton zygote-ookinete surface antigen of *Plasmodium berghei*. Infect Immun 1991;59(January (1)):36–44.
[24] Sinden RE. Molecular interactions between Plasmodium and its insect vectors. Cell Microbiol 2002;4:713–24.
[25] Aregawi M, Cibulskis R, Otten M, Williams R, Dye C. World Health Organisation, World Malaria Report; 2008.
[26] Wu Y, Ellis RD, Shaffer D, Fontes E, Malkin EM, Mahanty S, et al. Phase 1 trial of malaria transmission blocking vaccine candidates Pfs25 and Pvs25 formulated with montanide ISA 51. PLoS ONE 2008;3(7):e2636.
[27] Tsuboi T, Takeo S, Iriko H, Jin L, Tsuchimochi M, Matsuda S, et al. Wheat germ cell-free system-based production of malaria proteins for discovery of novel vaccine candidates. Infect Immun 2008;76(April (4)):1702–8.
[28] Yoshida S, Araki H, Yokomine T. Baculovirus-based nasal drop vaccine confers complete protection against malaria by natural boosting of vaccine-induced antibodies in mice. Infect Immun 2010;78(February (2)):595–602.
[29] Hisaeda H, Collins WE, Saul A, Stowers AW. Antibodies to *Plasmodium vivax* transmission-blocking vaccine candidate antigens Pvs25 and Pvs28 do not show synergism. Vaccine 2001;20(December (5–6)):763–70.
[30] Abe T, Hemmi H, Miyamoto K, Morhhshi S, Tamura H, Takaku S, et al. Imvolvement of the Toll-like receptor 9 signalling pathway in the induction of innate immunity by baculovirus. J Virol 2005;79:2847–58.
[31] Kaslow DC, Bathurst IC, Barr PJ. Malaria transmission-blocking vaccines. Trends Biotechnol 1992;10(11):388–91.
[32] Vermeulen AN, Ponnudurai T, Beckers PJ, Verhave JP, Smits MA, Meuwissen JH. Sequential expression of antigens on sexual stages of *Plasmodium falciparum* accessible to transmission-blocking antibodies in the mosquito. J Exp Med 1985;162(5):1460–76.
[33] LeBlanc R, Vasquez Y, Hannaman D, Kumar N. Markedly enhanced immunogenicity of a Pfs25 DNA-based malaria transmission-blocking vaccine by in vivo electroporation. Vaccine 2008;26(January (2)):185–92.
[34] Lobo CA, Dhar R, Kumar N. Immunization of mice with DNA-based Pfs25 elicits potent malaria transmission-blocking antibodies. Infect Immun 1999;67(April (4)):1688–93.

research articles Journal of proteome research

Immunoproteomics Profiling of Blood Stage *Plasmodium vivax* Infection by High-Throughput Screening Assays

Jun-Hu Chen,[†,‡,#] Jae-Wan Jung,[§] Yue Wang,[†,‡] Kwon-Soo Ha,[§] Feng Lu,[†] Chae Seung Lim,[∥] Satoru Takeo,[⊥] Takafumi Tsuboi,[*,⊥] and Eun-Taek Han[*,†]

Department of Parasitology, School of Medicine, Kangwon National University, Chunchon, Gangwon-do, Republic of Korea, Institute of Parasitic Diseases, Zhejiang Academy of Medical Sciences, Hangzhou, Zhejiang, People's Republic of China, Department of Molecular and Cellular Biochemistry, School of Medicine, Kangwon National University, Chunchon, Gangwon-do, Republic of Korea, Department of Laboratory Medicine, College of Medicine, Korea University, Seoul, Republic of Korea, Cell-free Science and Technology Research Center, and Venture Business Laboratory, Ehime University, Matsuyama, Ehime, Japan

Received July 9, 2010

Completed genome sequences and stage-specific transcriptomes of the intraerythrocytic developmental cycle of *Plasmodium vivax* offers the opportunity to profile immune responses against *P. vivax* infection using innovative screening approaches. To detect the immune responses to blood stage-specific proteins, we applied a protein array technology to screen the sera of vivax malaria patients. Herein, a set of genes from the *P. vivax* blood stage was cloned using the In-Fusion cloning method and expressed by a wheat germ cell-free system. A total of 94 open reading frames (ORFs) were cloned and 89 (95%, 89/94) proteins were expressed, which were screened with sera from *P. vivax*-infected patients and healthy individuals using protein arrays. A total of 18 (19.1%, 18/94) highly immunoreactive proteins were identified, including 7 well-characterized vivax vaccine candidates. The remaining 11 ORFs have not been previously described as immunologically reactive. These novel immunoproteomes of the vivax malaria blood stage will be further studied as potential vaccine candidates. In this first report, high-throughput screening assays have been applied to investigate blood stage-specific immunoproteomes from vivax malaria. These methods may be used to determine immunodominant candidate antigens from the *P. vivax* genome.

Keywords: antigen • immunoproteomics • *Plasmodium vivax* • protein microarray

Introduction

Malaria remains one of the leading causes of both morbidity and mortality of humans residing in tropical countries. *Plasmodium falciparum* is justifiably regarded as the greater menace because of its high levels of mortality and prevalence on the world's most malarious continent, Africa. However, malarial infection as a result of *Plasmodium vivax* threatens almost 40% of the world's population, resulting in 132–391 million clinical infections each year.[1] Resistance of malaria parasites to chemotherapeutic agents such as chloroquine is increasing, which highlights the critical need for an effective vaccine. However, an effective malaria vaccine has not been achieved to date.[2] Currently, almost all efforts to develop a malaria vaccine have focused on *P. falciparum*. For example, there are 23 *P. falciparum* vaccine candidates undergoing advanced clinical studies and only two *P. vivax* vaccine candidates being tested in preliminary (Phase I) clinical trials, with few others being assessed in preclinical studies. More investment and a greater effort toward the development of *P. vivax* vaccine components are required.[3]

In the blood stage of malaria, antibodies are likely to play a major role in protection through several mechanisms, including inhibition of parasite invasion, intraerythrocytic parasite blockage, and mononuclear cell-mediated inhibition.[4] Humoral immune responses against blood-stage antigens are an important component of naturally acquired immunity to malaria. On one hand, parasite proteins engaged in erythrocyte invasion are potential targets of protective antibody responses.[5] On the other hand, the blood stage of *Plasmodium* causes the many pathological manifestations associated with malaria infection, and thus proteins expressed during this stage should include promising candidates for a vaccine.[6] There are many putative

* To whom correspondence should be addressed. 1) Mailing address for E. T. Han: Department of Parasitology, School of Medicine, Kangwon National University, Hyoja2-dong, Chunchon, Gangwon-do 200–701, Republic of Korea. Tel., +82-33-250-7941; fax, +82-33-255-8809. E-mail: (E. T. Han) ethan@kangwon.ac.kr. 2) Mailing address for T. Tsuboi: Cell-free Science and Technology Research Center and Venture Business Laboratory, Ehime University, 3 Bunkyo-cho, Matsuyama, Ehime 790-8577, Japan. Tel. +81-89-927-8277; fax, +81-89-927-9941. E-mail: (T. Tsuboi) tsuboi@ccr.ehime-u.ac.jp.

† Department of Parasitology, Kangwon National University.

‡ Institute of Parasitic Diseases, Zhejiang Academy of Medical Sciences.

Present address: National Institute of Parasitic Diseases, Chinese Center for Disease Control and Prevention, Shanghai, China.

§ Department of Molecular and Cellular Biochemistry, Kangwon National University.

∥ Department of Laboratory Medicine, Korea University.

⊥ Cell-free Science and Technology Research Center and Venture Business Laboratory, Ehime University.

10.1021/pr100705g

Published on Web 10/16/2010

specific immunogenic antigens present in the malaria proteome, which are considered largely responsible for triggering the host immune response and thus have a high potential for the development of vaccines against malaria parasites.[7]

With the completion of genome sequences and stage-specific transcriptomes of the intraerythrocytic developmental cycle of *P. vivax*, a postgenomic era has begun and has opened the eyes of vaccine biologists to a new approach to vaccine design for the prevention of vivax malaria infections.[8−11] However, annotation and validation of thousands of genes remains difficult due to the lack of a methodology that enables the preparation of quality proteins in an efficient manner. There is an urgent need to accelerate the pace of discovery of new malaria vaccine candidates using innovative screening approaches. Reverse vaccinology and high-throughput genome-based screens are two interrelated techniques that hold much promise in this regard.[12−14] Reverse vaccinology is based on running algorithms of genomic information (genomics, proteomics, and transcriptomics) and can be used to mine the information contained in the blueprint of the malaria genome. In most cases, this new technology has identified treasure troves of novel vaccine candidates and diagnostic markers.[15−17] To pursue such an approach, the establishment of a repository of cloned genes and high-throughput production of malaria multidomain proteins in the folded state would be extremely helpful.[18−20] Recently, from our experience of expressing around 100 malaria genes using wheat germ cell-free system (WGCF), we learned that the recombinant falciparum malaria proteins synthesized are of high quality and, therefore, amenable for vaccine candidate assessment.[19]

In the present study, in silico data mining by comparative genomics combined with In-Fusion cloning methods, a WGCF expression system, and protein arrays were applied to high-throughput profiling antibody responses against putative immunoproteomes from blood stage *P. vivax* infection. These methods may aid in determining the immunogenicity of candidate antigens and the functional identification of the large number of unknown and hypothetical proteins in the *P. vivax* genome.

Experimental Procedures

Gene/Open Reading Frame (ORF) Selection. The putative immunoproteome of *P. vivax* (Supplementary Table 1) was selected according to specific sets of criteria and separated into eight categories. A total of 90 unique genes without introns were used for PCR amplification and In-Fusion cloning. The major category ($n = 43$) was a pattern of schizont stage-specific genes/proteins of *P. vivax* that were orthologous to putative vaccine targets or merozoite proteins of *P. falciparum* (Supplementary Figure 1).[21,22] The other categories included glycosyl-phosphatidylinositol (GPI) anchored proteins ($n = 10$), the merozoite surface protein 3 (MSP3) family ($n = 11$), the merozoite surface protein 7 (MSP7) family ($n = 11$), the Pv-fam-a family ($n = 5$), the reticulocyte binding protein (RBP) family ($n = 4$), exported proteins ($n = 4$), and other well-characterized *P. vivax* genes/proteins (known antigenicity or immunogenicity, $n = 2$).[9,10] Because the reliability of producing desired PCR products decreases as the length of the genomic DNA fragment increases, genes longer than 3000 bp were divided into multiple overlapping sections (90 genes, divided into 109 ORFs), with 45 nucleotide overlaps. Sequence information for *P. vivax* was derived from the *Plasmodium* database (PlasmoDB, http://www.plasmodb.org/plasmo/home.jsp).[23]

Preparation of Linearized Vectors. The pEU-E01-His-TEV-MCS-N2 (pEU, CellFree Sciences, Matsuyama, Japan) vector was used for In-Fusion cloning. The vector was first linearized by double digestion with restriction enzymes *Xho* I and *Bam*H I (Takara, Japan) and purified using a QIAquick PCR Purification Kit (QIAGEN, Valencia, CA) according to the manufacturer's instructions. The quality of the digestion products was determined by 1% agarose gel electrophoresis and the concentration of linearized vectors was measured using a Nanodrop ND-1000 Spectrophotometer (Nanodrop Technology, Rockland, DE).

PCR Amplification of ORFs. In-Fusion cloning allows for the joining of a vector and insert, as long as they share 15 bases of homology at each end. Therefore, In-Fusion PCR primers must be designed in such a way that they generate PCR products containing ends that are homologous to those of the vectors. Gene-specific primers were designed with Invitrogen OligoPerfect Designer (http://tools.invitrogen.com/content.cfm?pageid=9716). The nucleotide sequences for the signal peptide and the GPI anchor were excluded from the gene expression constructs.[24,25] Gene-specific primers were then converted into In-Fusion PCR primers with the In-Fusion Primer Design Tool (http://bioinfo.clontech.com/infusion/convertPcrPrimersInit.do). Each gene-specific sense and antisense primer was extended at the 5′-terminus with the sequence 5′-GGG CGG ATA TCT CGA G-3′ and 5′-GCG GTA CCC GGG ATC CTT A-3′, respectively.

Genomic DNA, a cDNA library, and ds cDNA of *P. vivax* were used for PCR amplification of target genes. Genomic DNA was prepared from 200 μL of whole blood from a *P. vivax* patient using QIAamp DNA Blood Mini Kits (QIAGEN), which provided 200 μL aliquots of template DNA. *P. vivax* ds cDNA and the cDNA library were prepared using a SMART cDNA synthesis kit (Clontech Laboratories, Inc., Mountain View, CA).

Each ORF was amplified in a 20 μL PCR reaction containing 0.5 U Platinum *Taq* DNA Polymerase High Fidelity (Invitrogen, Carlsbad, CA), 0.2 μM each of the sense and antisense primers, 1 μL of genomic DNA, 200 μM dNTPs, and $MgSO_4$ to a final concentration of 2.0 mM. The 109 gene targets were amplified in-parallel beginning with an initial denaturation at 94 °C for 2 min, followed by 35 cycles of 94 °C for 20 s, 60 °C for 30 s, and 68 °C for 3 min, then a final extension at 68 °C for 10 min. Unamplified targets were amplified in a 20 μL PCR reaction containing 0.4 U Phusion High-Fidelity DNA Polymerase (Finnzymes, Espoo, Finland), 0.5 μM each of the sense and antisense primers, 1 μL of cDNA library or ds cDNA (1:10 dilution), 200 μM dNTPs, and $MgCl_2$ to a final concentration of 1.5 mM, which began with an initial denaturation at 98 °C for 30 s, followed by 35 cycles of 98 °C for 10 s, 60 °C for 30 s, and 72 °C for 2 min, then a final extension at 72 °C for 10 min. The quality of each gene product was measured using 1% agarose gel electrophoresis and stained in an ethidium bromide solution. The PCR products were visualized on a UV transilluminator and images were scanned with an imaging system (Vilber Lourmat, France).

In-Fusion Cloning of PCR Products. High-quality PCR products achieved on an agarose gel as a single, dense band of DNA were treated with the Cloning Enhancer (Clontech). Otherwise, PCR products containing additional nonspecific backgrounds were isolated using NucleoSpin Extract II Kits (Clontech) and spin column-purification prior to cloning. The cloning enhancer-treated PCR product (2 μL) or purified PCR product (50−200 ng) and 100 ng of the linearized pEU vector

were mixed with In-Fusion Enzyme (Clontech) in the PCR tubes and incubated for 15 min at 37 °C, followed by 15 min at 50 °C. Solutions were then placed on ice. All reactions were diluted 1:5 with TE buffer (10 mM Tris·HCl, pH 8.0, 1 mM EDTA) and 5 μL was used to transform JM109 competent cells (Intron Biotech, Inc., Daejeon, Korea). Transformants were selected by plating on culture plates containing 15 mL of LB agar, supplemented with ampicillin (100 μg/mL), and incubated overnight at 37 °C.

Four colonies from each vector/insert combination were randomly picked and screened by PCR amplification. Positive colonies were selected for plasmid preparation using the Wizard *Plus* SV Minipreps DNA Purification System (Promega, Madison, WI) according to the manufacturer's instructions. Purified DNA was sequenced and analyzed using the DNAstar analysis software (DNASTAR, Inc., Madison, WI).

Highly purified plasmid DNA is required for *in vitro* transcription and subsequent translation. A target colony was selected for plasmid preparation using the Midi Plus Ultrapure plasmid extraction system (Viogene, Taipei, Taiwan) according to the manufacturer's instructions. Purified DNA was eluted in 20−50 μL of 0.1× TE buffer (10 mM Tris-HCl, pH 8.0, 1 mM EDTA) and the concentration was accessed by a Nanodrop ND-1000 Spectrophotometer.

Protein Expression and Western Blot. *P. vivax* proteins were expressed by a 1 mL WGCF system using the bilayer translation reaction method described previously.[19] The total fraction and supernatant of each sample was separated by sodium dodecyl sulfate polyacrylamide gel electrophoresis (SDS-PAGE) under reducing conditions. The separated proteins were transferred to 0.45 μm PVDF membranes (Millipore, Billerica, MA) in a semidry transfer buffer (50 mM Tris, 190 mM glycine, 3.5 mM SDS, 20% methanol) at a constant 400 mA for 40 min using a Semi-Dry Blotting System (ATTO Corp., Tokyo, Japan). After blocking with 5% skim milk in TBS/T, Penta·His antibody (QIAGEN) and secondary horseradish peroxidase (HRP)-conjugated goat anti-mouse IgG (Pierce) were used to detect His-tagged recombinant proteins. The immunoblots were incubated with enhanced chemiluminescence solution (EZ-ECL, GE Healthcare) for 1 min and exposed for 1 min to BioMax XAR film (Kodak) in a cassette. The results were documented by a Perfection 1260 Scanner (Epson). Crude protein samples were stored in aliquots at −80 °C until further use.

Several proteins were detected in 20 cases of pooled sera from vivax malaria patients and healthy individuals (1:200). Bound antibodies were detected by incubation in AP-conjugated anti-human IgG (1:2500, Sigma). The immunoblots were incubated with BCIP/NBT color development solution.

Preparation of Amine Arrays. Glass slides (75 × 25 mm) were cleaned with a solution of $H_2O_2/NH_4OH/H_2O$ (1:1:5, v/v) at 70 °C for 10 min, incubated with 1.5% 3-aminopropyltrimethoxysilane solution (v/v) in 95% ethanol for 2 h, and sequentially washed with ethanol and water. The amine-modified glass slides were dried under air gas and baked at 110 °C for 2 h. Teflon tapes with 200 holes (25 × 8) each and a 1.5 mm diameter were attached to the modified glass slides to prepare well-type amine arrays.[26]

Detection of His-Tagged Protein Expression Using Amine Arrays. One microliter of each crude *P. vivax* protein solution was spotted in duplicate to each well of the arrays and incubated for 2 h at 37 °C. In addition, the array contained an area spotted with purified PvCSP (expressed by the WGCF system) and wheat germ lysate without any plasmid vector, which were regarded as positive and negative controls, respectively. The array was first blocked with 5% BSA in PBS containing 0.1% Tween 20 (PBS-T) for 1 h at 37 °C and incubated with Penta·His antibody (1 μL, 10 ng/μL) in PBS-T for 1 h at 37 °C. Antibodies were visualized with Alexa Fluor 546 goat anti-mouse IgG (10 ng/μL, Invitrogen) in PBS-T for 1 h at 37 °C and scanned in a fluorescence scanner (ScanArray Express, PerkinElmer, Boston, MA).[27] Fluorescence intensities of array spots were quantified by the fixed circle method using ScanArray Express software version 4.0 (PerkinElmer). The positive cutoff value was calculated as the mean fluorescence intensity value of the negative controls plus two standard deviations (SD).

Enzyme-Linked Immunosorbent Assay (ELISA). To validate the immunoreactivity detected by the protein arrays, sera from 20 cases of vivax malaria and 10 healthy individuals were tested against a well-characterized vivax blood stage antigen PvMSP1-19 (expressed by WGCF system) by ELISA as described previously.[28] The positive sera samples of vivax malaria were collected from patients (mean age, 35 yr; range 18−60 yr) with the symptoms and positive (mean parasitemia, 0.148%; range 0.036−0.630%) for vivax malaria by microscopy at Korea University Ansan Hospital, local health centers and clinics in Gyeonggi and Gangwon Provinces in endemic areas of the Republic of Korea. In addition, the sera samples of healthy individuals, negative by microscopy, were collected in nonendemic areas of the Republic of Korea. The positive cutoff value was calculated as the mean optical density (OD) value of the normal controls plus 2 SD. The sera were screened by protein arrays as follows.

Serum Screening Using Arrays. Sera from 20 cases of vivax malaria and 10 healthy individuals were screened by well-type amine arrays. Briefly, 1 μL of antibody solution (10 ng/μL in 9.3 mM phosphate buffer, pH 7.4) was spotted to each well of the arrays and incubated for 2 h at 37 °C. Then, 1 μL of each crude *P. vivax* protein solution was spotted in duplicate to each well of the arrays and incubated for 1 h at 37 °C. In addition, the arrays contained an area spotted with purified PvMSP1-19 as a positive control and wheat germ lysate without any plasmid vector as a negative control. For all staining, the array was first blocked with 5% BSA in PBS-T for 1 h at 37 °C. Then, the chips were probed with human serum (1:200) that was first preabsorbed against wheat germ lysate (1:100) to block anti-wheat germ antibodies. Bound antibodies were visualized with Alexa Fluor 546 goat anti-human IgG (10 ng/μL, Invitrogen) in PBS-T and quantified as described above. The response by a particular serum sample was considered positive overall if the relative ratio of signal intensity (SI) was >2.0 (test relative to negative control >2.0) and the response was statistically significant ($p < 0.05$) compared to the negative control SI.

After primary screening of the human sera, 18 proteins with high immunoreactivity were screened again with sera from these 20 cases of vivax malaria and 10 healthy individuals together on one well-type array.

Statistical Analysis. Differences between the means of each group were analyzed for statistical significance with Excel software using a two-tailed unpaired Student *t*-tests. Differences in proportions were compared using a χ^2 test. Statistical differences of $p < 0.05$ were considered significant. The Benjamini-Hochberg method was used to correct for the false discovery rate using MULTTEST procedure in version 8.0 of SAS/STAT software.[15] The correlation between duplicate spots of the protein arrays, and antibody reactivity of different

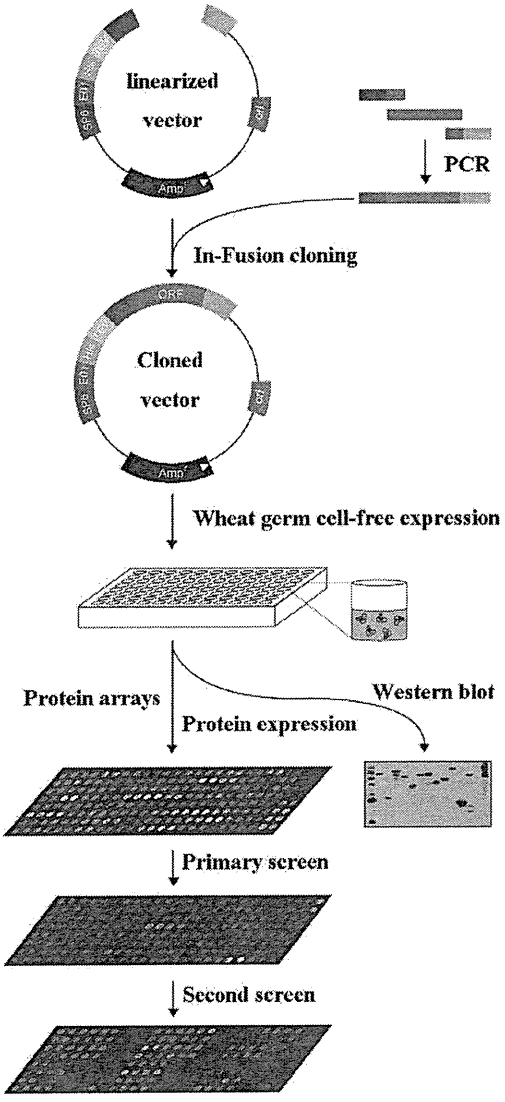

Figure 1. Schematic representation of overall procedures. The genes of interest were amplified by PCR and the PCR products were cloned into a pEU vector. The resulting plasmids were directly used as expression templates for wheat germ cell-free protein expression, and expression efficiency was analyzed by Western blot and protein arrays. Then, all of the expressed proteins were spotted on one array and screened with serum from *P. vivax* infected patients and healthy individuals. Subsequently, individual candidate protein with high immunoreactivity was spotted on one array and screened with individual serum from vivax malaria patients and healthy individuals.

concentrations of the recombinant proteins was analyzed using Origin software, version 6.1 (OriginLab Corp., Northampton, MA) or GraphPad Prism software, version 5.0 (GraphPad, San Diego, CA). The hierarchical cluster of gene expression and antibody responses was calculated and drawn using the TIGR multiarray experiment viewer (MeV) software.[29]

Results

PCR Amplification of ORFs and In-Fusion Cloning. Procedures for the PCR amplification and In-Fusion gene cloning are outlined in Figure 1. Polymerases with proofreading characteristics were used for PCR amplification to increase the quality of the PCR products, because the nonspecific PCR

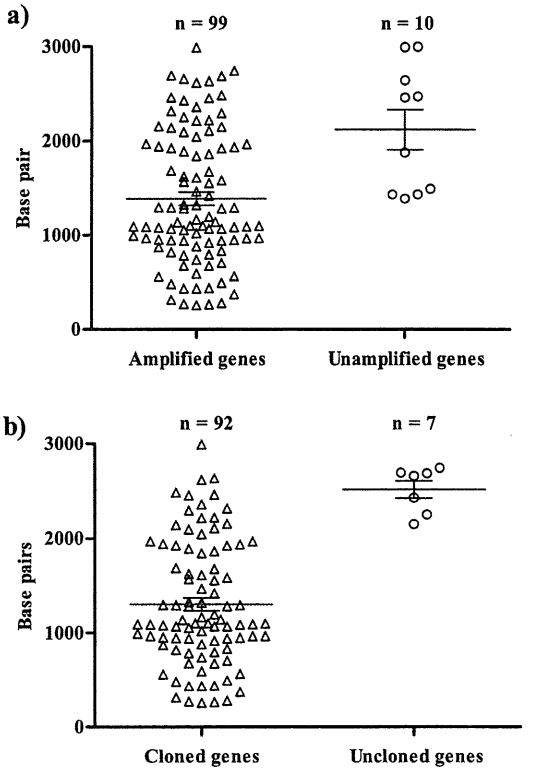

Figure 2. PCR amplification and In-Fusion cloning of *P. vivax* genes. (a) Size distribution of amplified and unamplified *P. vivax* ORFs by PCR amplification was significantly different ($p < 0.01$). (b) Size distribution of cloned and uncloned *P. vivax* ORFs by In-Fusion cloning was significantly different ($p < 0.001$). The horizontal lines to the right of the data points are the mean and the upper and lower 95% confidence limits.

products or primer dimers might hinder the efficiency of cloning. From a total of 109 *P. vivax* ORFs selected for PCR amplification, 99 amplified ORFs with an average size of 1390 bp were significantly shorter than 10 unamplified ORFs with an average size of 2123 bp (independent samples *t*-test, two-tailed, $p < 0.01$) (Figure 2a). Among the 10 unamplified ORFs, 9 belonged to the MSP3 ($n = 6$) and RBP ($n = 3$) gene families, which may contribute to a large size or degree of polymorphism of target ORFs.[30]

Four colonies per transformation were picked at random for screening by colony PCR to evaluate the efficiency of In-Fusion cloning. The screening results showed that, of the 99 ORFs screened, 92 were successfully cloned (92.9%) with an average size of 1304 bp and 7 ORFs were unsuccessfully cloned with an average size of 2518 bp. Statistical analyses indicated that the cloned ORFs were significantly shorter in length than the uncloned ORFs (independent samples *t*-test, two-tailed, $p < 0.001$) (Figure 2b). To collect more ORFs, two ORFs were cloned after screening 16 randomly selected colonies per ORF from the 7 uncloned ORFs.

High-Throughput Expression of *P. vivax* Proteins. Most targets were expressed using the WGCF system, as shown by an obvious band on the SDS-PAGE gel (data not shown). The recombinant N-terminal His_6-tag fusion proteins were detected by Western blot with Penta·His antibody specific for the His_6-tag epitope of these His_6-tagged fusion proteins. These results demonstrate that 86 of the 94 ORFs (91.5%) yielded protein products (Figure 3). Eight constructs, all hypothetical genes, did not express any protein. Ninety percent (77/86) of the

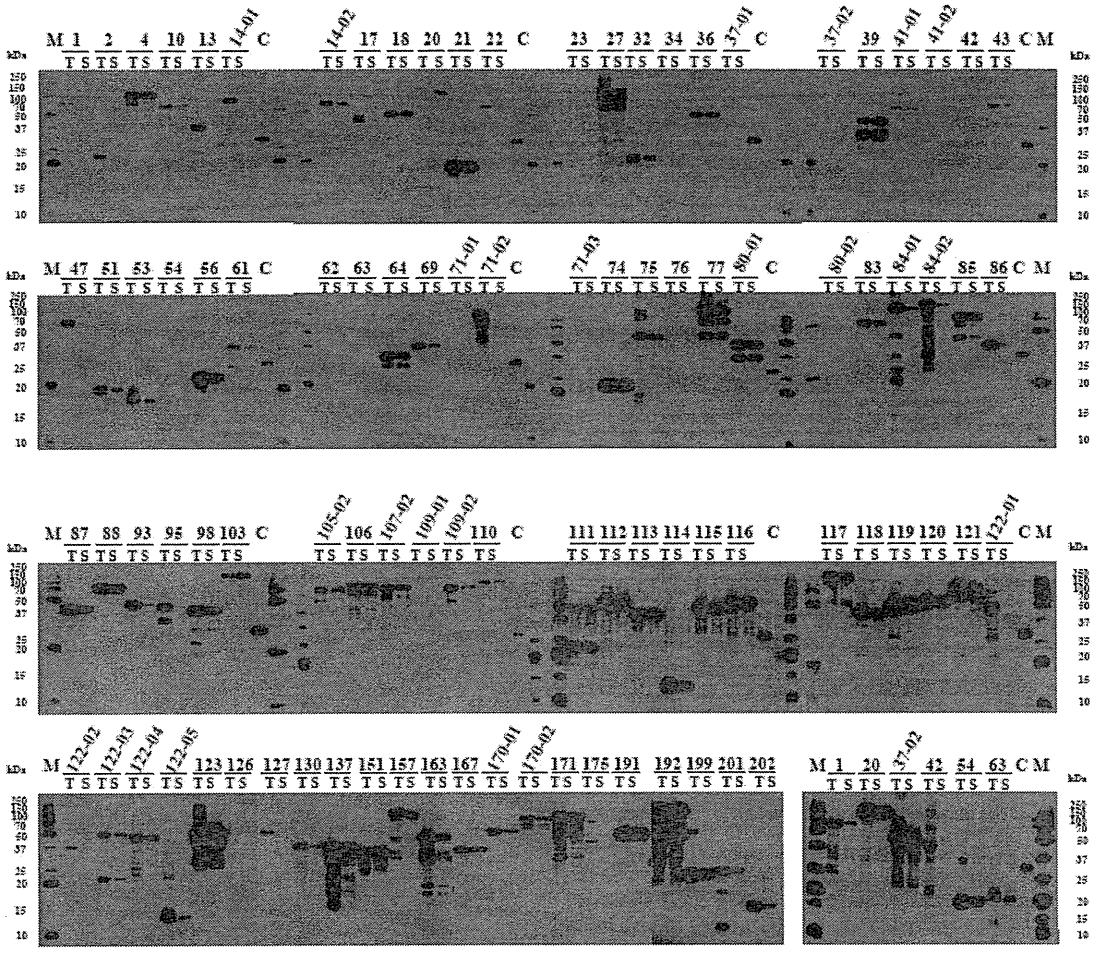

Figure 3. Western blot analysis of the expression levels and solubility of *P. vivax* proteins. Ninety-four proteins with two paired lanes (left, total fraction (T) and right, soluble fraction (S), the supernatant after centrifugation). Several samples (nos. 1, 20, 37-02, 42, 54, and 63) in the last panel were analyzed by Western blot a second time. M, Protein size marker; C, PvCSP proteins.

targets among the expressed proteins provided soluble fractions. Many proteins migrated differently than expected and that has been reported for a variety of proteins expressed by the WGCF system.[31]

High-Throughput analysis of *P. vivax* Protein Expression by Protein Arrays. We evaluated the efficiency of *P. vivax* protein expression with the Penta·His antibody by comparing protein arrays with Western blots (Figure 4a). The detection limit was approximately 10 ng for the protein arrays and 95% (89/94) of the *P. vivax* proteins were positive for the His_6-tags on the array. It was a novel concentration-dependent analysis method that showed a correlation coefficient of 0.99 between fluorescence intensities and protein concentrations ($p < 0.001$) (Figure 4b). When relative intensities of duplicate spots were plotted against each other, the resulting diagonal indicated good reproducibility of the spotting and detection of the immobilized proteins with a correlation coefficient of 0.93 ($p < 0.001$) (Figure 4c).

Antibody Profiling. The antibody response to PvMSP1-19 was determined for 20 vivax malaria patients and 10 healthy individuals by ELISA, as well as protein array (Supplementary Figure 2). Antibody reactivity against the PvMSP1-19 by ELISA was correlated with antibody reactivity measured against PvMSP1-19 on the array ($R^2 = 0.76$, $p < 0.001$) (data not shown). Moreover, antibody reactivity against the purified PvMSP1-19 (spotted on the array as a positive control) and the crude PvMSP1-19 generated in the high-throughput system was highly correlated ($R^2 = 0.83$, $p < 0.001$) (data not shown). The efficiency of protein arrays for antibody profiling was also evaluated using purified PvMSP1-19 (Supplementary Figure 3). A concentration-dependent analysis method showed a correlation coefficient of 0.97 between fluorescence intensities and protein concentration ($p < 0.001$). *P. vivax* protein arrays were probed with sera from 20 subjects who were naturally exposed to vivax malaria, and 10 subjects who were healthy individuals. Two protein arrays displaying the entire target protein probed with serum from a healthy individual and a vivax malaria patient are shown in Figure 5, panels a and b, respectively. Sera from malaria-naïve subjects showed low reactivity (Figure 5a), whereas sera from *P. vivax*-exposed individuals showed obvious reactivity against WGCF expressed proteins (Figure 5b). After primary screening of human sera, proteins with high immunoreactivity were screened again with individual serum samples from patients and healthy individuals together on one array (Figure 5c). When relative intensities of duplicate spots were plotted against each other, the resulting diagonal indicated good reproducibility of the spotting and detection of the

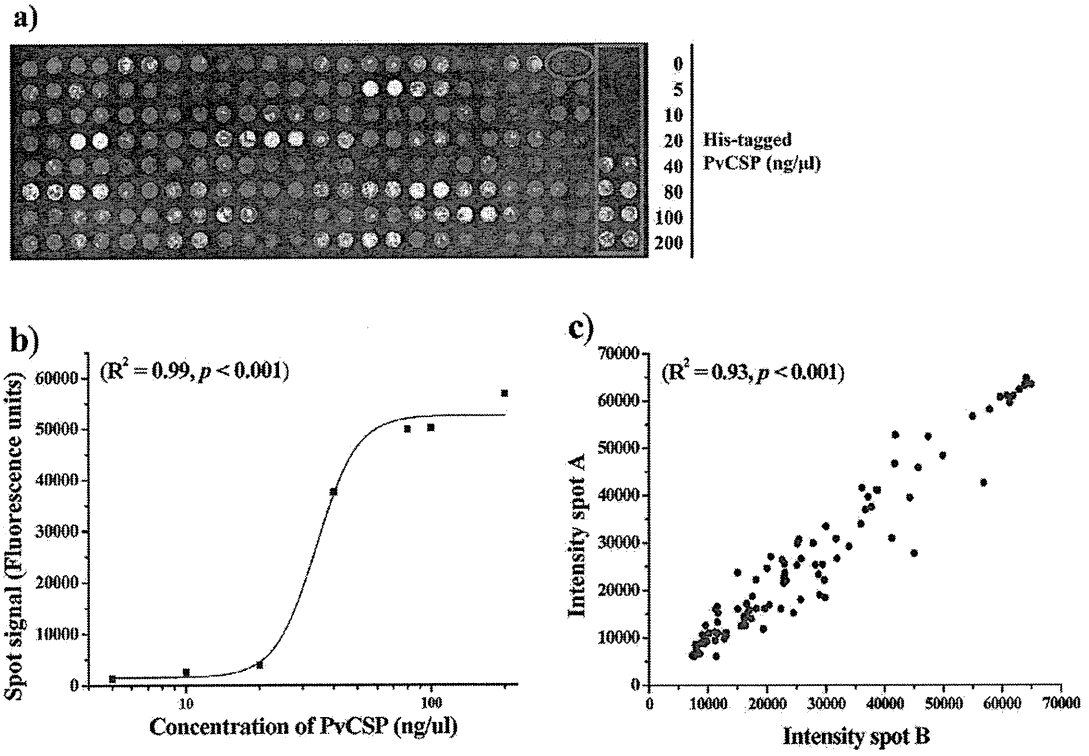

Figure 4. Analysis of *P. vivax* protein expression by protein arrays. (a) Protein arrays probed with anti-His_6-tag antibody. (b) Correlation between spot intensities and the serial diluted purified His-tagged PvCSP protein. (c) Correlation of relative spot intensities of duplicates (spot A versus its duplicate spot B). Control reactions of wheat germ lysate that lacked vector template (circle) and reactions of purified His-tagged PvCSP protein (rectangular box).

immobilized proteins with a high correlation coefficient (R^2 = 0.97, $p < 0.001$) (Figure 5b and d).

The Immunogenic Profiles of Human Sera Against *P. vivax* Proteins. A total of 30 and 7 arrays for primary and second screens were tested with sera from 20 vivax malaria patients and 10 healthy individuals, respectively, which displayed different patterns of immunoreactivity. The profiles of immunoreactivity against 18 ORFs (19.1% of total target proteins) representing the immunogenic antigens are shown in Figure 6a, in which the signal intensities for reactivity of each antigen by individual serum samples are shown in a colorized matrix. Three of the 18 most immunoreactive proteins are well-characterized *P. vivax* antigens, including AMA1 (PVX_092275), MSP1-42 (PVX_099980), and MSP1-19. These proteins are all leading vivax malaria vaccine candidates. MSP1-42 was recognized by all 20 cases of vivax malaria patient sera. Four GPI-anchored proteins (MSP1-19, MSP10 [PVX_114145], MSP8 [PVX_097625], and Pv12 [PVX_113775]), one 6-cysteine domain protein Pv41 (PVX_000995), two MSP3 proteins (MSP3.6 [PVX_097695], MSP3.9 [PVX_097710]), one MSP7 protein (MSP7 [PVX_082680]), one exported protein (ETRAMP 11.2, PVX_003565)), one hypothetical protein (PVX_087140), and AMA1 were recognized with ≥2 cases of vivax malaria patient sera (Table 1 and Supplementary Table 2). In addition, two MSP3 proteins (MSP3.3 [PVX_097680] and MSP3.7 [PVX_097700]), one MSP7 protein (PVX_082655), and three other hypothetical proteins (PVX_081550, PVX_090210, and PVX_094920) were recognized by serum from one patient. Most of these proteins have not been previously described as immunologically reactive. Interestingly, the ETRAMP 11.2 that was recognized by 14 cases in all of the 20 patient sera using protein arrays was also recognized by pooled patient sera using Western blots (Figure 7).

We analyzed the *P. vivax* microarray data through the asexual erythrocytic cycle for expression of genes encoding immunogenic proteins.[10] We found that 16 of these show an expression pattern consistent with involvement in invasion or schizonts stages, peaking in transcription TP6–TP9 postinvasion (Figure 6b). Only MSP8 has a flatter expression profile in the ring and trophozoite stage (TP1–TP6). In *P. falciparum*, *msp8* is associated with the establishment of early rings,[32] whereas it is transcribed throughout the ring and trophozoite stages, thus, reflecting an extended requirement for this protein in *P. vivax*.

Discussion

The reverse vaccinology approach has shown promise in spite of the essential requirement to generate hundreds of recombinant molecules for screening. As genomes are completed that contain thousands of genes each, more cost-effective and less time-consuming efforts to produce these clones will be needed. The In-Fusion cloning method, which is based on the In-Fusion enzyme, could be used in combination with any 15 bp homology region to enable ligation-independent cloning of PCR products to any linearized vector.[33] Previous studies have shown that constructs are suitable for expressing proteins from multiple hosts, that is, a single vector capable of expression in *Escherichia coli*, mammalian cell lines (e.g., HEK293T cells), and insect cell lines (e.g., Sf9 cells).[34]

We used In-Fusion cloning methods to construct a total of 92 vectors from 99 PCR products of *P. vivax* by colony PCR

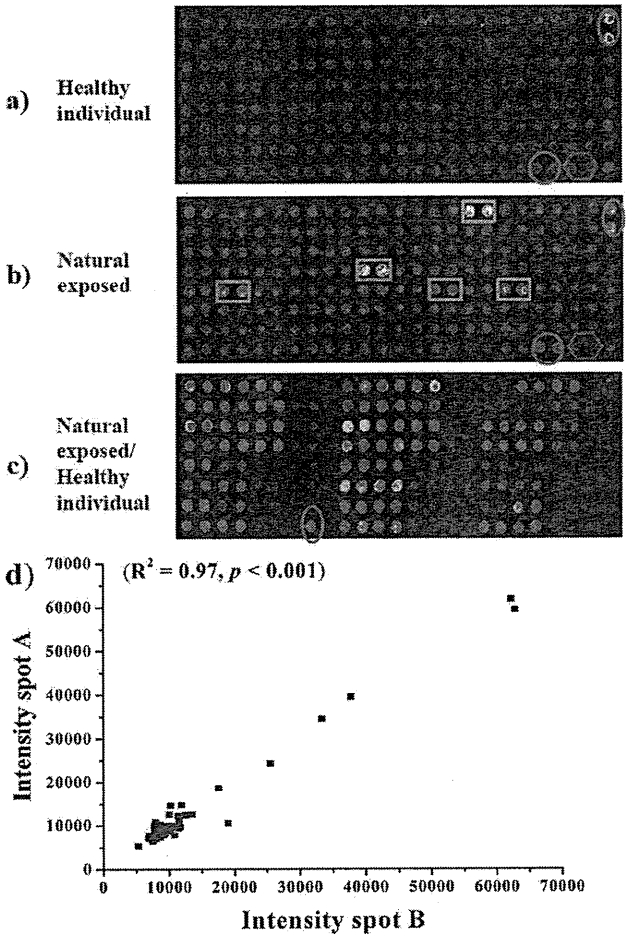

Figure 5. Antibody profiling of *P. vivax* proteins by protein arrays. (a) Crude *P. vivax* proteins react with individual healthy serum and (b) individual naturally exposed serum. Wheat germ lysate that lacked vector template (hexagons) and purified PvMSP1-19 (circles) probed with individual healthy serum served as inner negative and positive controls, respectively. Purified PvMSP1-19 (ellipses) reacted with pooled patient sera served as the outer positive control. Positive reactions with target proteins are marked with boxes. (c) Proteins with high immunoreactivity were screened again with sera from these 20 cases of vivax malaria patients and 10 healthy individuals together on one array. (d) Correlation of relative spot intensities of duplicates (spot A versus its duplicate spot B) from panel b.

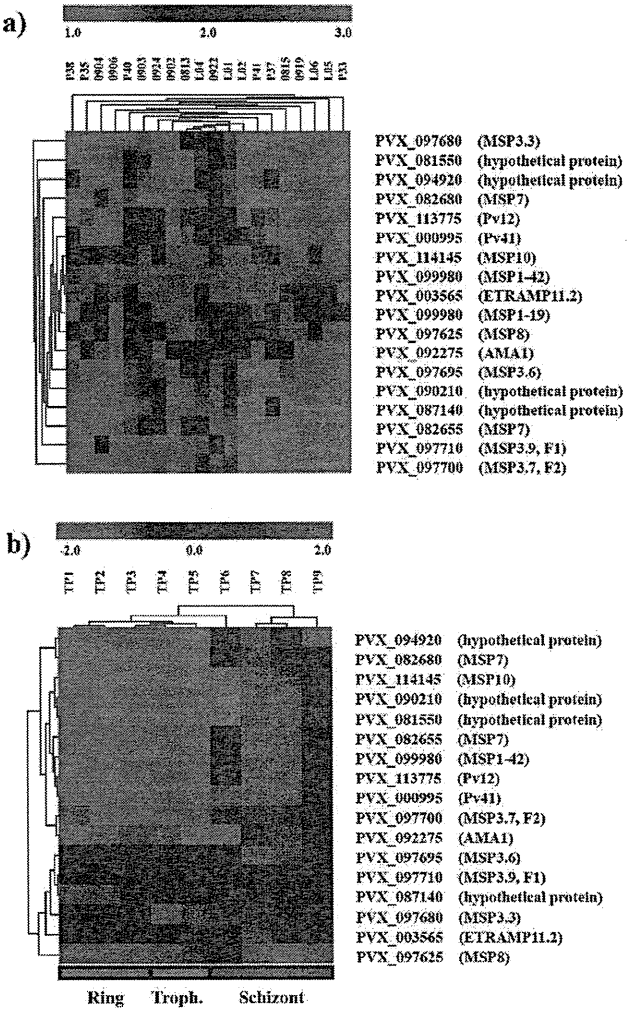

Figure 6. Immunoreactivity profiles and transcription patterns of immunogenic proteins of *P. vivax*. A total 18 antigens (17 genes) exhibit high IgG antibody responses to *P. vivax*-infected patient sera. (a) Immunoreactivity profiles of 18 immunogenic proteins. F1 and F2, fragment 1 and 2. (b) Transcription pattern of 17 genes coded immunogenic proteins. The transcription data of *P. vivax* genes were collected from microarray results.

screening of 4 randomly selected colonies. We had an overall cloning efficiency of 93%, which is similar to the cloning results of OPPF (e.g., 94%).[34] The results compare favorably with data reported by other studies examining high-throughput construction of expression vectors of *P. falciparum* using the Gateway recombination system (e.g., 84% PCR product to expression clone efficiency),[14] but similar to the *in vivo* recombination rate (e.g., 97%) in *E. coli*.[20] However, it is obvious that the In-Fusion cloning method is the most straightforward system for PCR cloning.[35]

E. coli-based expression systems have been widely used for the expression of malaria proteins; however, it is difficult to efficiently produce many proteins due to the complexity of the malaria genome. The immense drawback during high-level protein expression in *E. coli* is the production of insoluble proteins in inclusion bodies even if some proteins are successfully expressed,[36] and *Plasmodium* proteins have proven to be no exception. One thousand ORFs from *P. falciparum* have been tested using *E. coli* protein expression systems.[37] Of these, 337 proteins were expressed, although they were typically insoluble; 63 of the expressed proteins were soluble.[37] In contrast, Tsuboi et al.[38] attempted to express 500 of *P. falciparum* molecules belonging to sporozoite, merozoite, and gametocyte stages in a high-throughput format by the WGCF system. Eighty-four percent of them yielded soluble protein products. The biochemical, immunocytochemical, and biological analyses of the produced falciparum proteins have also demonstrated that the recombinant malaria proteins synthesized by this system are of high quality.[19,38] In *P. falciparum*, 93 of the 124 genes (75%) have yielded protein product. In the present study, 91.4% (86/94) of the genes of *P. vivax* were expressed by the WGCF protein synthesis system. The percentage of expressed proteins by the plasmid-based WGCF system was much higher than PCR-based methods the previously published protein expression of *P. falciparum*.[19] One possible explanation for the higher success rate is that the present study used the plasmid based transcriptional templates with higher

Table 1. Features of *P. vivax* Immunogenic Proteins and Their Homologues in *P. falciparum*

Pv gene ID	annotation	no. of positive (%)[a]	SP[b]	TMD[c]	features in *P. vivax*	features in homologues of *P. falciparum*
PVX_099980	MSP1-42	20 (100)	+	+	Vaccine candidate, GPI-AP	Vaccine candidate
PVX_003565	ETRAMP 11.2	14 (70)	+	+	Unknown	Antigenicity
PVX_099980	MSP1-19	13 (65)	+	+	Vaccine candidate, GPI-AP	Vaccine candidate
PVX_097625	MSP8	12 (60)	+	+	Antigenicity, GPI-AP	Antigenicity
PVX_114145	MSP10	9 (45)	+	−	Antigenicity, GPI-AP	Antigenicity
PVX_092275	AMA1	7 (35)	−	+	Vaccine candidate	Vaccine candidate
PVX_000995	Pv41	4 (20)	+	−	Antigenicity, Cys6 family	Antigenicity
PVX_113775	Pv12	3 (15)	+	+	Unknown, GPI-AP, Cys6 family	Antigenicity
PVX_087140	hypothetical	3 (15)	+	−	Unknown	Unknown
PVX_097695	MSP3.6	2 (10)	+	−	Unknown	Vaccine candidate
PVX_097710	MSP3.9	2 (10)	−	−	Unknown	Vaccine candidate
PVX_082680	MSP7	2 (10)	+	+	Unknown	Antigenicity
PVX_097680	MSP3.3	1 (5)	+	−	MSP3-beta, coiled coil	Vaccine candidate
PVX_097700	MSP3.7	1 (5)	−	−	Unknown	Vaccine candidate
PVX_082655	MSP7	1 (5)	+	−	Unknown	Antigenicity
PVX_081550	hypothetical	1 (5)	+	−	Unknown	Unknown
PVX_090210	hypothetical	1 (5)	+	−	Unknown	Unknown
PVX_094920	hypothetical	1 (5)	+	−	Unknown	Unknown

[a] Total number of positive antibody reaction with 20 patients serum samples. [b] SP, signal peptide. [c] TMD, transmembrane domain.

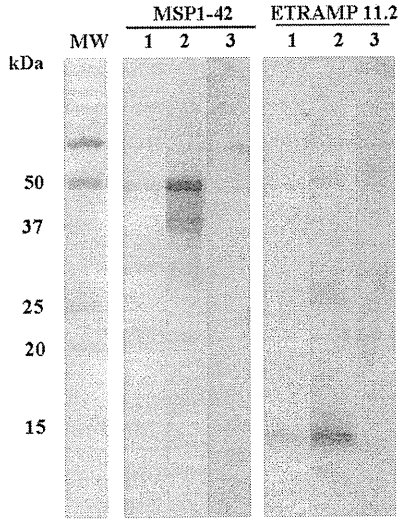

Figure 7. Western blot analysis of immunogenic proteins. Crude proteins were reacted with anti-His antibody (lane, 1), pooled patient serum (2), but not reacted with pooled healthy serum (3).

performance in contrast to the PCR based transcription templates used in the previous study.[19] Another explanation is that the genes from *P. vivax* have lower A/T contents (58%) rather than those of *P. falciparum* (76% in average). Whatever the reason, this study clearly demonstrated that the WGCF system is a suitable system for easily achieving high-throughput, high-solubility, and high-productivity in the whole-proteome-scale synthesis of *P. vivax* proteins in addition to that of *P. falciparum*.

In recent years, high-throughput genomics has provided blueprints for numerous genomes, thus, paving the way for major breakthroughs in biomedicine. Inspired by these advances, proteomics has become a key discipline for addressing protein expression patterns and for understanding the function and regulation of entire sets of proteins encoded by an organism.[39] Antibody-based microarrays are among the novel classes of rapidly evolving technologies with great potential for high-throughput proteomics.[40] Here, using protein arrays, we developed a high-throughput method for the analysis of His-tag fusion protein expression. The detection limit was 2.5 times more sensitive than Western blot analysis. Ninety-five percent (89/94) of *P. vivax* proteins were detected, consistent with that of Western blot (91%, 86/94).

The ability of microarrays to detect specific antibody responses to multiple antigens in parallel has significant clinical and research implications.[41] This methodology has already been shown to be useful in the serodiagnosis of infectious diseases.[13,15,16,42] Microarray analysis to obtain antibody reactivity profiles has also been shown to be useful in vaccine development against other organisms.[43,44] Recently, protein microarrays were used to characterize antibody reactivity profiles of *P. falciparum* infection.[20,45,46] From a panel of 250 putative *P. falciparum* proteins screened by protein microarrays, a total of 72 highly immunoreactive proteins were identified, including 16 well-characterized and 56 uncharacterized antigens.[20] Overall, 14 novel antigens were identified as potential target antigens for a subunit malaria vaccine.

In the present study, protein arrays were used to characterize antibody reactivity profiles of *P. vivax* infection. From a panel of 94 putative immunogenic proteins from the *P. vivax* blood stage screened by protein arrays, 18 (19.1%, 18/94) highly immunoreactive proteins were identified, including 3 well-characterized vivax vaccine candidates (AMA1, MSP1-42, and MSP1-19). MSP1-42 was recognized by IgG antibody in all 20 cases of *P. vivax*-infected patient sera, whereas AMA1 and MSP1-19 were only recognized by IgG antibody in 7−13 cases of *P. vivax*-infected patient sera. The major reason for this observation is that the expression levels of both recombinant AMA1 and MSP1-19 was not as high as the recombinant MSP1-42.

Three GPI-anchored proteins (MSP8, MSP10, and Pv12) were recognized by IgG antibody in *P. vivax*-infected patient sera by protein arrays. MSP8 and MSP10 were recently identified and the recombinant proteins were highly recognized by *P. vivax* infected patient sera.[47,48] In contrast to the apical and peripheral classes of blood stage antigens, the GPI-anchored proteins appear to be essential for blood-stage growth. Together with considerable data highlighting their potential as targets of antibodies, these results place the merozoite GPI-anchored

proteins among the most highly validated blood-stage vaccine targets.[21] MSP8 and MSP10 contain C-terminal double epidermal growth factor (EGF)-like modules in *P. vivax* and *P. falciparum* parasites.[9] Replacing PfMSP1 EGFs with the corresponding double EGF module from PvMSP8 or PvMSP10 may uncover the function of the (EGF)-like modules.[49]

Pv12- and Pv41-containing Cys_6 domains belong to the P230 proteins family. Pv12 has not been characterized, whereas Pv41 is expressed in parasite asexual stages and recognized by anti-rabbit serum raised against Pv41 peptide.[50] The P230 protein family is unique to *Plasmodium* species. A search of the complete *P. falciparum* genome sequence identified 10 genes conforming to the characteristics of this family, comprising 4 that are expressed in sexual stages (Pfs230, Pfs230p, Pfs48/45 and Pfs47), 3 in asexual stages (Pf12, Pf38 and Pf41), and the remaining 3 (Pfs36, Pfs36p and Pfs12p) of in sporozoite.[51] In *P. falciparum*, Pf12-GFP fusion protein was localized to the merozoite surface and Pf12 fusion protein expressed in *P. falciparum* was strongly recognized by antibodies present in individuals naturally exposed to *P. falciparum*.[52] Pf12 displays remarkably broad expression across the different life stages, which is expressed strongly in schizont, gametocyte, and sporozoite stages. Not only does this raise interesting questions about the potential broad nature of the biological function of such surface proteins, but it also suggests that a recombinant form of a single protein may have potential as a blood-stage, transmission-blocking and pre-erythrocytic vaccine.[52] The Pv12 gene is expressed in asexual stages,[10] but needed the confirmation Pv12 protein expression pattern.

P. vivax MSP3α (MSP3.10), MSP3β (MSP3.3), and MSP3γ (MSP3.1), of the MSP3 family that includes 11 members, have been characterized and are associated with but not anchored in the merozoite membrane.[9,10] All three proteins have an alanine-rich domain with heptad repeats that are predicted to form coiled-coil tertiary structures, which mediate protein–protein interactions.[53,54] With the exception of the well-known protein MSP3.3, three new MSP3 proteins (MSP3.6, MSP3.7, and MSP3.9) were recognized by IgG antibody in *P. vivax*-infected patient sera. Another MSP7 family also included 11 members and expression of the MSP7 protein (PVX_082695) was identified in *P. vivax* asexual blood stages and confirmed by immunofluorescence assay.[55] Two other previously unidentified MSP7 proteins (PVX_082680 and PVX_082655) were recognized by IgG antibody in *P. vivax*-infected patient sera using protein arrays.

ETRAMP 11.2 protein (PVX_003565) was recognized by IgG antibody in 70% of *P. vivax*-infected patient sera in this study. In *P. vivax, etramp* 11.2 are expressed in schizonts. Variation in the development of the parasitophorous vacuole due to the delay of *exp* and *etramp* gene expression might contribute to differences in erythrocyte modifications and lead to the observed differences in rigidity and cytoadherence between *P. vivax* and *P. falciparum*.[10]

Conclusion

We demonstrate that the In-Fusion cloning system provides a highly efficient method for producing recombinant expression plasmids containing genes from *P. vivax*. Most proteins were successfully expressed using a wheat germ cell-free protein synthesis system. Analysis of serum reactivity profiles using protein arrays offers an opportunity to assess antibody responses to malarial antigens in a high-throughput manner, and 18 novel immunogenic proteins of vivax malaria blood stage were identified that will be further studied as potential candidates for subunit vaccines. This is the first time that high-throughput screening assays have been used to investigate the immune responses to stage-specific proteins from the vivax malaria blood stage. These methods can be used to determine immunogenicity of candidate antigens from the *P. vivax* genome.

Abbreviations: WGCF, wheat germ cell-free; EGF, epidermal growth factor; MSPs, merozoite surface proteins; GPI, glycosylphosphatidylinositol; ORF, open reading frame; HT, high-throughput; ELISA, enzyme-linked immunosorbent assay.

Acknowledgment. We thank Kana Kato, Rie Sekito, and Miyuki Yano for their technical assistance. This work was supported by a Korean Science and Engineering Foundation (KOSEF) grant funded by the Korea Government (MOST) (No. R01-2007-000-11260-0) and National Research Foundation of Korea Grant funded by the Korean Government (2009-075103). This work was also supported in part by Grants-in-Aid from the Ministry of Health, Labour and Welfare, Japan (H20-shinkou-ippan-013 and H21-chikyukibo-ippan-005).

Supporting Information Available: Supplementary Table 1, characteristics of putative immunogenic proteins from the *P. vivax* blood stage. Supplementary Table 2, antibody response to immunogenic proteins from the *P. vivax* blood stage. Supplementary Figure 1, transcriptome of the putative immunoproteome of vivax malaria blood stage. A total of 90 genes (82 genes with transcriptome data) were selected for In-Fusion cloning. SP, signal peptide; TMD, transmembrane domain. The transcription data of *P. vivax* genes were collected from microarray results. Supplementary Figure 2, antibody response against PvMSP1-19 recombinant protein. (a) Antibody response against purified PvMSP1-19 by ELISA in sera from *P. vivax* infected patients ($n = 20$) and healthy individuals ($n = 10$). Supplementary Figure 3, antibody profiling of *P. vivax* proteins by protein arrays. (a) Purified PvMSP1-19 (conc., 0, 5, 10, 20, 40, 80, 200, and 400 ng/μL, from top to bottom) probed with pooled human sera (patient, pooled patient sera; control, pooled negative serum). (b) Correlation between spot intensities and the concentration of purified PvMSP1-19. This material is available free of charge via the Internet at http://pubs.acs.org.

References

(1) Price, R. N.; Tjitra, E.; Guerra, C. A.; Yeung, S.; White, N. J.; Anstey, N. M. Vivax malaria: neglected and not benign. *Am. J. Trop. Med. Hyg.* **2007**, *77* (6 Suppl.), 79–87.
(2) Mueller, I.; Galinski, M. R.; Baird, J. K.; Carlton, J. M.; Kochar, D. K.; Alonso, P. L.; del Portillo, H. A. Key gaps in the knowledge of *Plasmodium vivax*, a neglected human malaria parasite. *Lancet Infect. Dis.* **2009**, *9* (9), 555–66.
(3) Herrera, S.; Corradin, G.; Arevalo-Herrera, M. An update on the search for a *Plasmodium vivax* vaccine. *Trends Parasitol.* **2007**, *23* (3), 122–8.
(4) Richie, T. L.; Saul, A. Progress and challenges for malaria vaccines. *Nature* **2002**, *415* (6872), 694–701.
(5) King, C. L.; Michon, P.; Shakri, A. R.; Marcotty, A.; Stanisic, D.; Zimmerman, P. A.; Cole-Tobian, J. L.; Mueller, I.; Chitnis, C. E. Naturally acquired Duffy-binding protein-specific binding inhibitory antibodies confer protection from blood-stage *Plasmodium vivax* infection. *Proc. Natl. Acad. Sci. U.S.A.* **2008**, *105* (24), 8363–8.
(6) Waters, A. Malaria: new vaccines for old. *Cell* **2006**, *124* (4), 689–93.
(7) Beeson, J. G.; Osier, F. H.; Engwerda, C. R. Recent insights into humoral and cellular immune responses against malaria. *Trends Parasitol.* **2008**, *24* (12), 578–84.

(8) Winzeler, E. A. Malaria research in the post-genomic era. *Nature* **2008**, *455* (7214), 751–6.
(9) Carlton, J. M.; Adams, J. H.; Silva, J. C.; Bidwell, S. L.; Lorenzi, H.; Caler, E.; Crabtree, J.; Angiuoli, S. V.; Merino, E. F.; Amedeo, P.; Cheng, Q.; Coulson, R. M.; Crabb, B. S.; Del Portillo, H. A.; Essien, K.; Feldblyum, T. V.; Fernandez-Becerra, C.; Gilson, P. R.; Gueye, A. H.; Guo, X.; Kang'a, S.; Kooij, T. W.; Korsinczky, M.; Meyer, E. V.; Nene, V.; Paulsen, I.; White, O.; Ralph, S. A.; Ren, Q.; Sargeant, T. J.; Salzberg, S. L.; Stoeckert, C. J.; Sullivan, S. A.; Yamamoto, M. M.; Hoffman, S. L.; Wortman, J. R.; Gardner, M. J.; Galinski, M. R.; Barnwell, J. W.; Fraser-Liggett, C. M. Comparative genomics of the neglected human malaria parasite *Plasmodium vivax*. *Nature* **2008**, *455* (7214), 757–63.
(10) Bozdech, Z.; Mok, S.; Hu, G.; Imwong, M.; Jaidee, A.; Russell, B.; Ginsburg, H.; Nosten, F.; Day, N. P.; White, N. J.; Carlton, J. M.; Preiser, P. R. The transcriptome of *Plasmodium vivax* reveals divergence and diversity of transcriptional regulation in malaria parasites. *Proc. Natl. Acad. Sci. U.S.A.* **2008**, *105* (42), 16290–5.
(11) Westenberger, S. J.; McClean, C. M.; Chattopadhyay, R.; Dharia, N. V.; Carlton, J. M.; Barnwell, J. W.; Collins, W. E.; Hoffman, S. L.; Zhou, Y.; Vinetz, J. M.; Winzeler, E. A. A systems-based analysis of *Plasmodium vivax* lifecycle transcription from human to mosquito. *PLoS Negl. Trop. Dis.* **2010**, *4* (4), e653.
(12) Rappuoli, R.; Covacci, A. Reverse vaccinology and genomics. *Science* **2003**, *302* (5645), 602.
(13) Davies, D. H.; Liang, X.; Hernandez, J. E.; Randall, A.; Hirst, S.; Mu, Y.; Romero, K. M.; Nguyen, T. T.; Kalantari-Dehaghi, M.; Crotty, S.; Baldi, P.; Villarreal, L. P.; Felgner, P. L. Profiling the humoral immune response to infection by using proteome microarrays: high-throughput vaccine and diagnostic antigen discovery. *Proc. Natl. Acad. Sci. U.S.A.* **2005**, *102* (3), 547–52.
(14) Aguiar, J. C.; LaBaer, J.; Blair, P. L.; Shamailova, V. Y.; Koundinya, M.; Russell, J. A.; Huang, F.; Mar, W.; Anthony, R. M.; Witney, A.; Caruana, S. R.; Brizuela, L.; Sacci, J. B., Jr.; Hoffman, S. L.; Carucci, D. J. High-throughput generation of *P. falciparum* functional molecules by recombinational cloning. *Genome Res.* **2004**, *14* (10B), 2076–82.
(15) Felgner, P. L.; Kayala, M. A.; Vigil, A.; Burk, C.; Nakajima-Sasaki, R.; Pablo, J.; Molina, D. M.; Hirst, S.; Chew, J. S.; Wang, D.; Tan, G.; Duffield, M.; Yang, R.; Neel, J.; Chantratita, N.; Bancroft, G.; Lertmemongkolchai, G.; Davies, D. H.; Baldi, P.; Peacock, S.; Titball, R. W. A *Burkholderia pseudomallei* protein microarray reveals serodiagnostic and cross-reactive antigens. *Proc. Natl. Acad. Sci. U.S.A.* **2009**, *106* (32), 13499–504.
(16) Zhu, H.; Hu, S.; Jona, G.; Zhu, X.; Kreiswirth, N.; Willey, B. M.; Mazzulli, T.; Liu, G.; Song, Q.; Chen, P.; Cameron, M.; Tyler, A.; Wang, J.; Wen, J.; Chen, W.; Compton, S.; Snyder, M. Severe acute respiratory syndrome diagnostics using a coronavirus protein microarray. *Proc. Natl. Acad. Sci. U.S.A.* **2006**, *103* (11), 4011–6.
(17) Steller, S.; Angenendt, P.; Cahill, D. J.; Heuberger, S.; Lehrach, H.; Kreutzberger, J. Bacterial protein microarrays for identification of new potential diagnostic markers for *Neisseria meningitidis* infections. *Proteomics* **2005**, *5* (8), 2048–55.
(18) Berrow, N. S.; Alderton, D.; Owens, R. J. The precise engineering of expression vectors using high-throughput In-Fusion PCR cloning. *Methods Mol. Biol.* **2009**, *498*, 75–90.
(19) Tsuboi, T.; Takeo, S.; Iriko, H.; Jin, L.; Tsuchimochi, M.; Matsuda, S.; Han, E. T.; Otsuki, H.; Kaneko, O.; Sattabongkot, J.; Udomsangpetch, R.; Sawasaki, T.; Torii, M.; Endo, Y. Wheat germ cell-free system-based production of malaria proteins for discovery of novel vaccine candidates. *Infect. Immun.* **2008**, *76* (4), 1702–8.
(20) Doolan, D. L.; Mu, Y.; Unal, B.; Sundaresh, S.; Hirst, S.; Valdez, C.; Randall, A.; Molina, D.; Liang, X.; Freilich, D. A.; Oloo, J. A.; Blair, P. L.; Aguiar, J. C.; Baldi, P.; Davies, D. H.; Felgner, P. L. Profiling humoral immune responses to *P. falciparum* infection with protein microarrays. *Proteomics* **2008**, *8* (22), 4680–94.
(21) Cowman, A. F.; Crabb, B. S. Invasion of red blood cells by malaria parasites. *Cell* **2006**, *124* (4), 755–66.
(22) Bozdech, Z.; Llinas, M.; Pulliam, B. L.; Wong, E. D.; Zhu, J.; DeRisi, J. L. The transcriptome of the intraerythrocytic developmental cycle of *Plasmodium falciparum*. *PLoS Biol.* **2003**, *1* (1), E5.
(23) Aurrecoechea, C.; Brestelli, J.; Brunk, B. P.; Dommer, J.; Fischer, S.; Gajria, B.; Gao, X.; Gingle, A.; Grant, G.; Harb, O. S.; Heiges, M.; Innamorato, F.; Iodice, J.; Kissinger, J. C.; Kraemer, E.; Li, W.; Miller, J. A.; Nayak, V.; Pennington, C.; Pinney, D. F.; Roos, D. S.; Ross, C.; Stoeckert, C. J., Jr.; Treatman, C.; Wang, H. PlasmoDB: a functional genomic database for malaria parasites. *Nucleic Acids Res.* **2009**, *37* (Database issue), D539–43.
(24) Eisenhaber, B.; Bork, P.; Eisenhaber, F. Prediction of potential GPI-modification sites in proprotein sequences. *J. Mol. Biol.* **1999**, *292* (3), 741–58.
(25) Bendtsen, J. D.; Nielsen, H.; von Heijne, G.; Brunak, S. Improved prediction of signal peptides: SignalP 3.0. *J. Mol. Biol.* **2004**, *340* (4), 783–95.
(26) Jung, J. W.; Jung, S. H.; Yoo, J. O.; Suh, I. B.; Kim, Y. M.; Ha, K. S. Label-free and quantitative analysis of C-reactive protein in human sera by tagged-internal standard assay on antibody arrays. *Biosens. Bioelectron.* **2009**, *24* (5), 1469–73.
(27) Park, J. Y.; Jung, S. H.; Jung, J. W.; Kwon, M. H.; Yoo, J. O.; Kim, Y. M.; Ha, K. S. A novel array-based assay of in situ tissue transglutaminase activity in human umbilical vein endothelial cells. *Anal. Biochem.* **2009**, *394* (2), 217–22.
(28) Mehrizi, A. A.; Zakeri, S.; Salmanian, A. H.; Sanati, M. H.; Djadid, N. D. IgG subclasses pattern and high-avidity antibody to the C-terminal region of merozoite surface protein 1 of *Plasmodium vivax* in an unstable hypoendemic region in Iran. *Acta Trop.* **2009**, *112* (1), 1–7.
(29) Saeed, A. I.; Sharov, V.; White, J.; Li, J.; Liang, W.; Bhagabati, N.; Braisted, J.; Klapa, M.; Currier, T.; Thiagarajan, M.; Sturn, A.; Snuffin, M.; Rezantsev, A.; Popov, D.; Ryltsov, A.; Kostukovich, E.; Borisovsky, I.; Liu, Z.; Vinsavich, A.; Trush, V.; Quackenbush, J. TM4: a free, open-source system for microarray data management and analysis. *BioTechniques* **2003**, *34* (2), 374–8.
(30) Rayner, J. C.; Huber, C. S.; Feldman, D.; Ingravallo, P.; Galinski, M. R.; Barnwell, J. W. Plasmodium vivax merozoite surface protein PvMSP-3 beta is radically polymorphic through mutation and large insertions and deletions. *Infect. Genet. Evol.* **2004**, *4* (4), 309–19.
(31) Goshima, N.; Kawamura, Y.; Fukumoto, A.; Miura, A.; Honma, R.; Satoh, R.; Wakamatsu, A.; Yamamoto, J.; Kimura, K.; Nishikawa, T.; Andoh, T.; Iida, Y.; Ishikawa, K.; Ito, E.; Kagawa, N.; Kaminaga, C.; Kanehori, K.; Kawakami, B.; Kenmochi, K.; Kimura, R.; Kobayashi, M.; Kuroita, T.; Kuwayama, H.; Maruyama, Y.; Matsuo, K.; Minami, K.; Mitsubori, M.; Mori, M.; Morishita, R.; Murase, A.; Nishikawa, A.; Nishikawa, S.; Okamoto, T.; Sakagami, N.; Sakamoto, Y.; Sasaki, Y.; Seki, T.; Sono, S.; Sugiyama, A.; Sumiya, T.; Takayama, T.; Takayama, Y.; Takeda, H.; Togashi, T.; Yahata, K.; Yamada, H.; Yanagisawa, Y.; Endo, Y.; Imamoto, F.; Kisu, Y.; Tanaka, S.; Isogai, T.; Imai, J.; Watanabe, S.; Nomura, N. Human protein factory for converting the transcriptome into an in vitro-expressed proteome. *Nat. Methods* **2008**, *5* (12), 1011–7.
(32) Drew, D. R.; Sanders, P. R.; Crabb, B. S. Plasmodium falciparum merozoite surface protein 8 is a ring-stage membrane protein that localizes to the parasitophorous vacuole of infected erythrocytes. *Infect. Immun.* **2005**, *73* (7), 3912–22.
(33) Hartley, J. L. Cloning technologies for protein expression and purification. *Curr. Opin. Biotechnol.* **2006**, *17* (4), 359–66.
(34) Berrow, N. S.; Alderton, D.; Sainsbury, S.; Nettleship, J.; Assenberg, R.; Rahman, N.; Stuart, D. I.; Owens, R. J. A versatile ligation-independent cloning method suitable for high-throughput expression screening applications. *Nucleic Acids Res.* **2007**, *35* (6), e45.
(35) Lu, Q. Seamless cloning and gene fusion. *Trends Biotechnol.* **2005**, *23* (4), 199–207.
(36) Yokoyama, S. Protein expression systems for structural genomics and proteomics. *Curr. Opin. Chem. Biol.* **2003**, *7* (1), 39–43.
(37) Mehlin, C.; Boni, E.; Buckner, F. S.; Engel, L.; Feist, T.; Gelb, M. H.; Haji, L.; Kim, D.; Liu, C.; Mueller, N.; Myler, P. J.; Reddy, J. T.; Sampson, J. N.; Subramanian, E.; Van Voorhis, W. C.; Worthey, E.; Zucker, F.; Hol, W. G. Heterologous expression of proteins from *Plasmodium falciparum*: results from 1000 genes. *Mol. Biochem. Parasitol.* **2006**, *148* (2), 144–60.
(38) Tsuboi, T.; Takeo, S.; Arumugam, T. U.; Otsuki, H.; Torii, M. The wheat germ cell-free protein synthesis system: a key tool for novel malaria vaccine candidate discovery. *Acta Trop.* **2010**, *114* (3), 171–6.
(39) Wingren, C.; Ingvarsson, J.; Dexlin, L.; Szul, D.; Borrebaeck, C. A. Design of recombinant antibody microarrays for complex proteome analysis: choice of sample labeling-tag and solid support. *Proteomics* **2007**, *7* (17), 3055–65.
(40) Ramachandran, N.; Raphael, J. V.; Hainsworth, E.; Demirkan, G.; Fuentes, M. G.; Rolfs, A.; Hu, Y.; LaBaer, J. Next-generation high-density self-assembling functional protein arrays. *Nat. Methods* **2008**, *5* (6), 535–8.
(41) Parekh, F. K.; Richie, T. L. Characterization of immune reactivity profiles using microarray technology may expedite identification of candidate antigens for next generation malaria vaccines. *Clin. Chem.* **2007**, *53* (7), 1183–5.
(42) Mezzasoma, L.; Bacarese-Hamilton, T.; Di Cristina, M.; Rossi, R.; Bistoni, F.; Crisanti, A. Antigen microarrays for serodiagnosis of infectious diseases. *Clin. Chem.* **2002**, *48* (1), 121–30.
(43) Li, B.; Jiang, L.; Song, Q.; Yang, J.; Chen, Z.; Guo, Z.; Zhou, D.; Du, Z.; Song, Y.; Wang, J.; Wang, H.; Yu, S.; Wang, J.; Yang, R. Protein

microarray for profiling antibody responses to *Yersinia pestis* live vaccine. *Infect. Immun.* **2005**, *73* (6), 3734–9.
(44) Gray, J. C.; Corran, P. H.; Mangia, E.; Gaunt, M. W.; Li, Q.; Tetteh, K. K.; Polley, S. D.; Conway, D. J.; Holder, A. A.; Bacarese-Hamilton, T.; Riley, E. M.; Crisanti, A. Profiling the antibody immune response against blood stage malaria vaccine candidates. *Clin. Chem.* **2007**, *53* (7), 1244–53.
(45) Sundaresh, S.; Doolan, D. L.; Hirst, S.; Mu, Y.; Unal, B.; Davies, D. H.; Felgner, P. L.; Baldi, P. Identification of humoral immune responses in protein microarrays using DNA microarray data analysis techniques. *Bioinformatics* **2006**, *22* (14), 1760–6.
(46) Crompton, P. D.; Kayala, M. A.; Traore, B.; Kayentao, K.; Ongoiba, A.; Weiss, G. E.; Molina, D. M.; Burk, C. R.; Waisberg, M.; Jasinskas, A.; Tan, X.; Doumbo, S.; Doumtabe, D.; Kone, Y.; Narum, D. L.; Liang, X.; Doumbo, O. K.; Miller, L. H.; Doolan, D. L.; Baldi, P.; Felgner, P. L.; Pierce, S. K. A prospective analysis of the Ab response to *Plasmodium falciparum* before and after a malaria season by protein microarray. *Proc. Natl. Acad. Sci. U.S.A.* **2010**, *107* (15), 6958–63.
(47) Perez-Leal, O.; Sierra, A. Y.; Barrero, C. A.; Moncada, C.; Martinez, P.; Cortes, J.; Lopez, Y.; Torres, E.; Salazar, L. M.; Patarroyo, M. A. Plasmodium vivax merozoite surface protein 8 cloning, expression, and characterisation. *Biochem. Biophys. Res. Commun.* **2004**, *324* (4), 1393–9.
(48) Perez-Leal, O.; Sierra, A. Y.; Barrero, C. A.; Moncada, C.; Martinez, P.; Cortes, J.; Lopez, Y.; Salazar, L. M.; Hoebeke, J.; Patarroyo, M. A. Identifying and characterising the *Plasmodium falciparum* merozoite surface protein 10 *Plasmodium vivax* homologue. *Biochem. Biophys. Res. Commun.* **2005**, *331* (4), 1178–84.
(49) Drew, D. R.; O'Donnell, R. A.; Smith, B. J.; Crabb, B. S. A common cross-species function for the double epidermal growth factor-like modules of the highly divergent *Plasmodium* surface proteins MSP-1 and MSP-8. *J. Biol. Chem.* **2004**, *279* (19), 20147–53.
(50) Angel, D. I.; Mongui, A.; Ardila, J.; Vanegas, M.; Patarroyo, M. A. The *Plasmodium vivax* Pv41 surface protein: identification and characterization. *Biochem. Biophys. Res. Commun.* **2008**, *377* (4), 1113–7.
(51) van Dijk, M. R.; van Schaijk, B. C.; Khan, S. M.; van Dooren, M. W.; Ramesar, J.; Kaczanowski, S.; van Gemert, G. J.; Kroeze, H.; Stunnenberg, H. G.; Eling, W. M.; Sauerwein, R. W.; Waters, A. P.; Janse, C. J. Three members of the 6-cys protein family of *Plasmodium* play a role in gamete fertility. *PLoS Pathog.* **2010**, *6* (4), e1000853.
(52) Sanders, P. R.; Gilson, P. R.; Cantin, G. T.; Greenbaum, D. C.; Nebl, T.; Carucci, D. J.; McConville, M. J.; Schofield, L.; Hodder, A. N.; Yates, J. R., III; Crabb, B. S. Distinct protein classes including novel merozoite surface antigens in Raft-like membranes of *Plasmodium falciparum*. *J. Biol. Chem.* **2005**, *280* (48), 40169–76.
(53) Galinski, M. R.; Corredor-Medina, C.; Povoa, M.; Crosby, J.; Ingravallo, P.; Barnwell, J. W. *Plasmodium vivax* merozoite surface protein-3 contains coiled-coil motifs in an alanine-rich central domain. *Mol. Biochem. Parasitol.* **1999**, *101* (1–2), 131–47.
(54) Galinski, M. R.; Ingravallo, P.; Corredor-Medina, C.; Al-Khedery, B.; Povoa, M.; Barnwell, J. W. Plasmodium vivax merozoite surface proteins-3beta and-3gamma share structural similarities with *P. vivax* merozoite surface protein-3alpha and define a new gene family. *Mol. Biochem. Parasitol.* **2001**, *115* (1), 41–53.
(55) Mongui, A.; Perez-Leal, O.; Soto, S. C.; Cortes, J.; Patarroyo, M. A. Cloning, expression, and characterisation of a *Plasmodium vivax* MSP7 family merozoite surface protein. *Biochem. Biophys. Res. Commun.* **2006**, *351* (3), 639–44.

PR100705G

Nozawa et al. BMC Biotechnology 2011, 11:35
http://www.biomedcentral.com/1472-6750/11/35

BMC Biotechnology

METHODOLOGY ARTICLE Open Access

Production and partial purification of membrane proteins using a liposome-supplemented wheat cell-free translation system

Akira Nozawa[1,2], Tomio Ogasawara[1,2], Satoko Matsunaga[1], Takahiro Iwasaki[1], Tatsuya Sawasaki[1,2,3*] and Yaeta Endo[1,2,3*]

Abstract

Background: Recently, some groups have reported on cell-free synthesis of functional membrane proteins (MPs) in the presence of exogenous liposomes (liposomes). Previously, we reported synthesis of a functional AtPPT1 plant phosphate transporter that was associated with liposomes during translation. However, it is unclear whether or not lipid/MP complex formation is common to all types of MPs in the wheat cell-free system.

Results: AtPPT1 was synthesized using a wheat cell-free system with or without liposomes. AtPPT1 synthesized with liposomes showed high transport activity, but the activity of AtPPT1 synthesized without liposomes was less than 10% activity of that with liposomes. To test whether co-translational association with liposomes is observed in the synthesis of other MPs, we used 40 mammalian MPs having one to 14 transmembrane domains (TMDs) and five soluble proteins as a control. The association rate of all 40 MPs into liposomes was more than 40% (mean value: 59%), while that of the five soluble proteins was less than 20% (mean value: 12%). There were no significant differences in association rate among MPs regardless of the number of TMDs and synthesis yield. These results indicate that the wheat cell-free system is a highly productive method for lipid/MP complex formation and is suitable for large-scale preparation. The liposome association of green fluorescent protein (GFP)-fusion MPs were also tested and recovered as lipid/MP complex after floatation by Accudenz density gradient ultracentrifugation (DGU). Employment of GFP-MPs revealed optimal condition for Accudenz floatation. Using the optimized Accudenz DGU condition, P2RX4/lipid complexes were partially purified and detected as a major band by Coomassie Brilliant Blue (CBB)-staining after SDS-PAGE.

Conclusion: Formation of lipid/AtPPT1 complex during the cell-free synthesis reaction is critical for synthesis of a functional MP. The lipid/MP complex during the translation was observed in all 40 MPs tested. At least 29 MPs, as judged by their higher productivity compared to GFP, might be suitable for a large-scale preparation. MPs synthesized by this method form lipid/MP complexes, which could be readily partially purified by Accudenz DGU. Wheat cell-free protein synthesis in the presence of liposomes will be a useful method for preparation of variety type of MPs.

* Correspondence: sawasaki@eng.ehime-u.ac.jp; yendo@eng.ehime-u.ac.jp
[1]Cell-Free Science and Technology Research Center and the Venture Business, Laboratory, Ehime University, 3 Bunkyo-Cho, Matsuyama, Ehime 790-8577, Japan
Full list of author information is available at the end of the article

Background

MPs comprise up to 30% of genes in fully sequenced genomes and have critical roles in a variety of biological processes including signal transduction, substrate transport, and energy production [1,2]. However, functional and structural studies of MPs are far behind that of soluble proteins. One of the major bottlenecks in the study of MPs is the difficulty in obtaining sufficient amounts of homogeneous protein. For instance, it is typically not easy to purify MPs in preparative scale, due to their low abundance in natural sources. Overexpression of recombinant MPs in living cells is often unsuccessful due to the inhibitory effect of high MP concentration on host cell physiology [3].

Recently, cell-free protein synthesis systems have emerged as a promising tool for MP production [4-6]. In addition to decoupling protein production from the toxic or inhibitory effects on host cell physiology, cell-free systems offer a unique advantage in that protein synthesis can be easily modified by addition of accessory elements, such as detergents and lipids. The addition of detergents and lipids to cell-free systems allows the synthesis of MP/detergent and MP/lipid complexes, respectively, and successful synthesis of functional MPs in this fashion have been reported recently [7-11]. For example, Klammt et al. [12] demonstrated that a G protein-coupled receptor, ETB, can be synthesized in a soluble form using an *Escherichia coli*-based cell-free system supplemented with Brij78, and that the synthesized proteins have ligand binding activity. The ligand binding activity of a human olfactory receptor, hOR17-4, synthesized using a wheat cell-free system in the presence of FC14, has been also reported [13]. Kalmbach et al. [14] reported that *E. coli* cell-free synthesized bacteriorhodopsin in the presence of liposomes was active in black lipid membrane mediated photocurrent measurements. Goren and Fox [15] showed reconstitution of the functional stearoyl Co-A desaturase complex, which consists of three proteins, cytochrome b_5, cytochrome b_5 reductase, and human stearoyl-CoA desaturase 1 (hSCD1) synthesized by wheat cell-free system in the presence of asolectin liposomes. However, the general versatility of this method is unclear as the above examples focus on specific MPs.

In a previous study, we reported functional synthesis of a phosphate trranslocator in a wheat cell-free synthesis system supplemented with liposomes and formation of lipid/MP complexes [16]. The mechanism for production of functional protein in this method is not clear, but association of synthesized MP with liposomes may be an important step. To better understand this, we tested the timing of liposome addition to the cell-free MP synthesis reaction. We also investigated whether other MPs synthesized by the method also associates with liposomes. Moreover, we tried to purify the synthesized MP as a lipid/MP complex by DGU.

Results and Discussion

Timing of liposome-supplementation to wheat cell-free translation system for synthesis of functional MPs

Previously, we reported synthesis and liposome association of functional MPs using a wheat cell-free system supplemented with liposomes [16]. To verify that co-translational association of MP with liposomes is critical for functional synthesis, we tested the synthesis of an *Arabidopsis thaliana* phosphate translocator, AtPPT1, in the presence of, absence of, and after post-translational addition of liposomes. These synthesized proteins were reconstituted into liposomes by freeze-thaw and sonication methods after mixing with substrate-preloaded liposomes and phosphate-incorporation activity was measured. Similar to a previous report [16], AtPPT1 synthesized in the absence of liposomes had only 4% of the activity of AtPPT1 synthesized in the presence of liposomes (Figure 1). AtPPT1 synthesized in the absence of liposomes was mixed post-translationally with liposomes and yielded 6% the activity of AtPPT1 synthesized in the presence of liposomes. The association of synthesized AtPPT1 with liposomes, either co- or post-translationally, was measured after sucrose DGU and

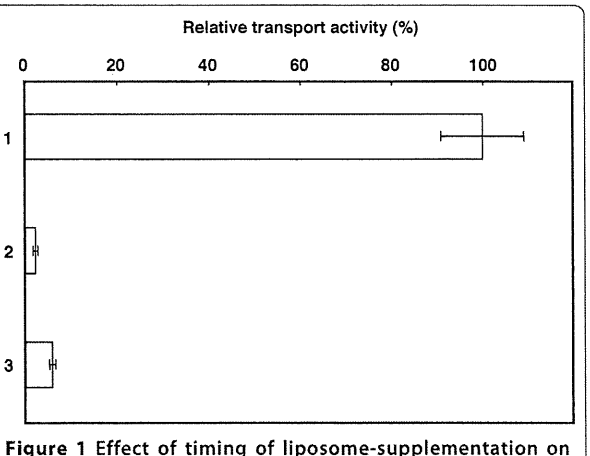

Figure 1 Effect of timing of liposome-supplementation on transport activity of synthesized AtPPT1. Three types of AtPPT1 proteins were prepared, 1: AtPPT1 synthesized with liposomes, 2: AtPPT1 synthesized without liposomes, 3: AtPPT1 synthesized without liposomes and mixed with liposomes post-synthesis. Each type of synthesis was reconstituted in liposomes that had been pre-loaded with 30 mM phosphate. Uptake of [^{32}P] phosphate into the liposomes was measured. The 100% exchange activity of the synthesized protein was 151 n mol/min/mg proteins. Data is reported as the mean±SD of values from three independent experiments.

showed no significant differences (50% co-translational, 62% post-translational). These results indicate that formation of lipid/AtPPT1 complex during the synthesis reaction is an important step for synthesizing functional AtPPT1. Supplementation of liposomes into the cell-free system would prevent aggregation and precipitation of AtPPT1 proteins during synthesis reaction. So, the constitution of AtPPT1/lipid complexes might be effective for formation of functional state MPs in the following freeze-thaw and sonication steps. For preparing MPs in functional state by cell-free system, preventing aggregation and precipitation of MPs during synthesis reaction by supplementation of lipids and/or detergents would be a critical point.

Cell-free synthesis of MPs in the presence of liposomes

Using a wheat cell-free system in the presence of liposomes, a plant MP, AtPPT1, was synthesized as a lipid/MP complex (Figure 1). As MPs account for more than 50% of all human drug targets [17], we wanted to understand if the AtPPT1 membrane association described above was applicable to mammalian MPs. In general, MPs are classified by the number of TMDs and to start we tested five human MPs ranging from 2 to 12 TMD (KCNJ8, 2TMD; GABRD, 4TMD; HTR2B, 7TMD; P2RY11, 7TMD; SLC22A7, 12TMD). The selected mammalian MPs were synthesized in the wheat cell-free system in the presence of asolectin liposomes and their liposome association rates were measured after sucrose DGU. In this experiment, mRNA was prepared from fragments made by split-primer PCR [18,19]. By using a PCR-based fragment as a template for *in vitro* transcription, time consuming steps, such as cloning of a target gene and construction of an expression vector were eliminated. Although the yield of template is low, this step allows for screening large numbers of proteins. As shown in Figure 2, every protein in the test set was associated with liposomes. After sucrose DGU, ^{14}C-labeled proteins were predominantly detected in bands six to eight (Figure 2A), which corresponded with the observed liposome bands [16]. For each fraction, the radioactivity was measured and the relative amount of radioactivity for each fraction is depicted in Figure 2B. The extent of association for these proteins ranged from 52 to 73%, when three fractions, numbers six to eight, were treated as liposome fractions. The observed MP association is similar to that seen AtPPT1 (58%). Also there were no significant differences in the extent of association between the five MPs having two to 12 TMDs. These results suggest that association of synthesized MPs with liposomes during wheat cell-free synthesis is as likely to occur in other MPs as was observed for AtPPT1.

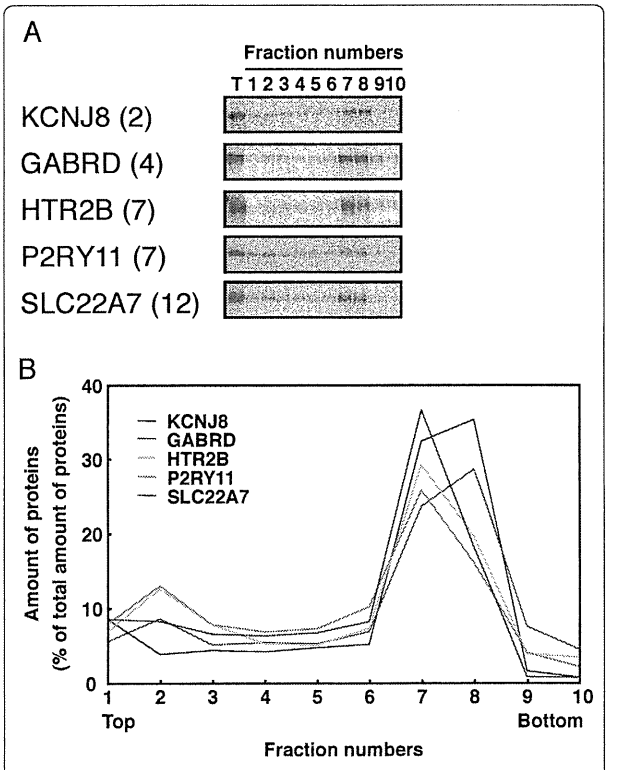

Figure 2 Association of synthesized MPs with liposomes. **(A)** SDS-PAGE analysis of liposome association of MPs. MPs were synthesized using a wheat cell-free system supplemented with liposomes and [^{14}C]-leucine. After the synthesis reaction, the reaction mixture was subjected to sucrose DGU and fractions were collected from the top of the tube. Synthesized proteins in each fraction were detected by SDS-PAGE and autoradiography. The number of TMDs of each protein is shown in parentheses. T means total fraction of reaction mixture. **(B)** Yield of synthesized proteins in each fraction. After fractionation, synthesized proteins were precipitated by 10% trichloroacetic acid and radioactivity of each fraction was measured by liquid scintillation counter.

Next we further analyzed membrane association using a larger set of proteins, which consisted of 29 human and 6 mouse MPs. While a majority of the test proteins were chosen at random, we ensured that there were multiple representatives of each tested MP family to examine synthesis yield and extent of liposome association within a family. As shown in Figure 3A, the 29 MPs tested showed better synthesis efficiency than GFP (not shown, 4.4 μg/150 μL reaction). The mean value of yield for the set of MPs was 5.9 μg/150 μL reaction. All tested proteins belonging to KCNJ, P2RX, GABR and SC5A families were well synthesized in the wheat cell-free system, whereas production of CACNG family proteins was very low (Figure 3B and Table 1). The remaining proteins, belonging to ENDR, P2RY, SLC6A and SLC22A families had both poorly and well synthesized proteins. (Figure 3B and Table 1).

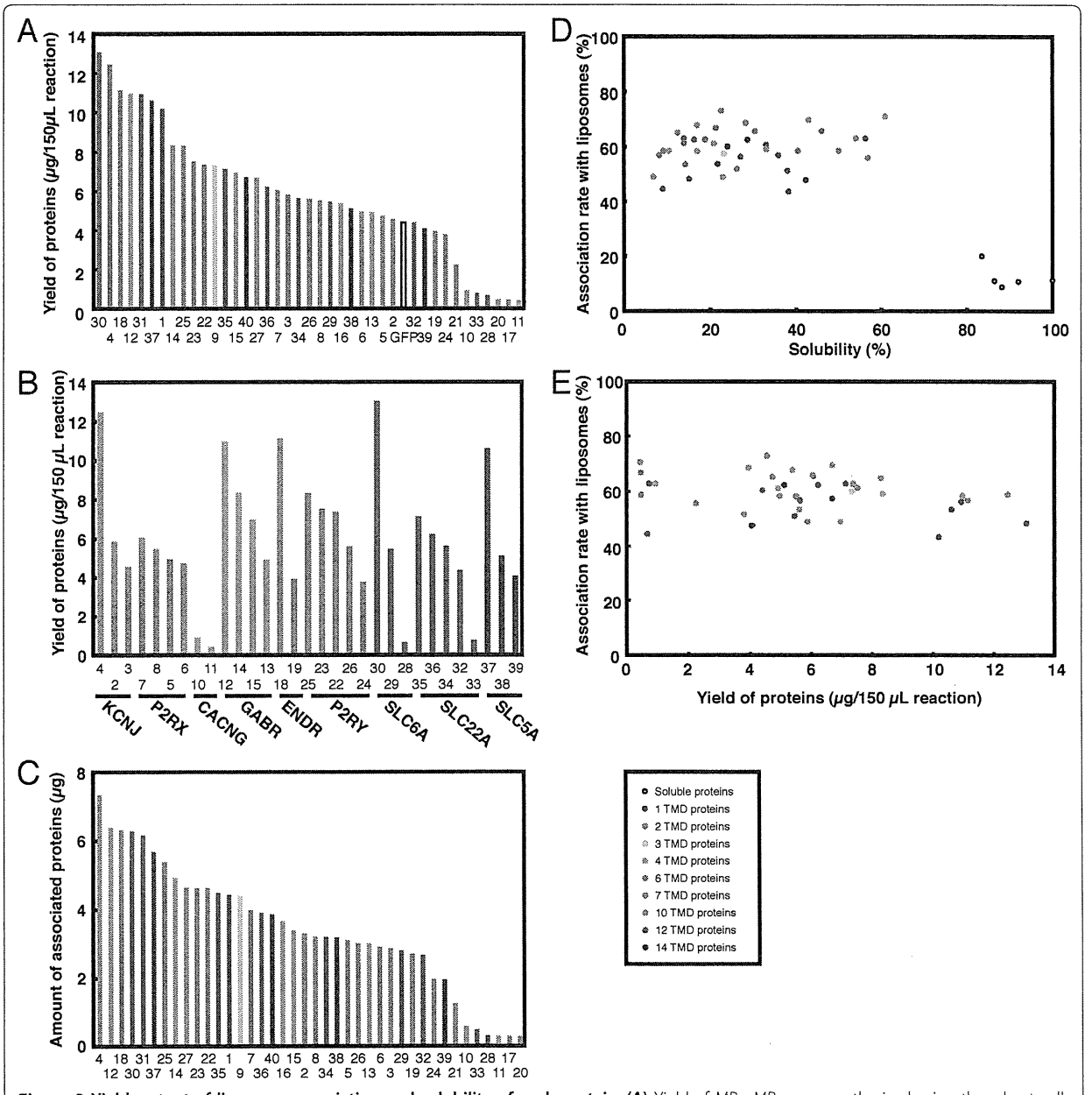

Figure 3 Yield, extent of liposome association and solubility of each protein. **(A)** Yield of MPs. MPs were synthesized using the wheat cell-free system supplemented with [^{14}C]-leucine and liposomes. Proteins were precipitated by 10% trichloroacetic acid and radioactivity was measured by liquid scintillation counter and the yield of each protein was calculated. The numbers on the x-axis correspond to the proteins in Table I. **(B)** Yield of MPs in each protein family. **(C)** Amount of liposome-associated proteins. MPs were synthesized using the wheat cell-free system supplemented with [^{14}C]-leucine and liposomes. After synthesis, the translation reaction was separated by sucrose DGU and fractions were collected from the top of the tube. The protein content of each fraction was estimated through radioactivity measurements of proteins precipitated by 10% trichloroacetic acid. The extent of association was calculated by combining the liposome fractions six through eight. For each protein, the specific amount of association with liposomes was calculated from the synthesis yield and extent of association. **(D)** The relationship between the extent of association and solubility of each protein. Membrane and soluble proteins were synthesized using the wheat cell-free system supplemented with or without liposomes and [^{14}C]-leucine. Proteins synthesized without liposomes were separated into soluble and insoluble fraction by centrifugation. The unprocessed synthesis reactions and the insoluble fractions were precipitated by 10% trichloroacetic acid and radioactivity was measured by liquid scintillation counter to determine the solubility for each protein. The extent of association for soluble proteins was calculated using the same method as for MPs. The extent of association and solubility of membrane and soluble proteins are plotted. **(E)** Relationship between extent of association and yield for each protein. Values for the extent of association and yield of each protein are plotted.